Title

Structural and fluid evolution of a young accretionary complex: The Hoh rock assemblage of the western Olympic Peninsula, Washington

Journal

Geological Society of America Bulletin, 105(8)

ISSN

0016-7606

Authors

ORANGE, DANIEL L
GEDDES, DUNCAN S
MOORE, J CASEY

Publication Date

1993-08-01

DOI

10.1130/0016-7606(1993)105<1053:safeoa>2.3.co;2

Peer reviewed

Structural and fluid evolution of a young accretionary complex: The Hoh rock assemblage of the western Olympic Peninsula, Washington

DANIEL L. ORANGE*
DUNCAN S. GEDDES
J. CASEY MOORE
Department of Earth Sciences and *Institute of Tectonics, University of California, Santa Cruz, California 95064*

ABSTRACT

The Hoh rock assemblage of the western Olympic Peninsula, Washington, was deposited in Eocene to Miocene time, and accreted, deformed, uplifted, and eroded by the late Miocene. Northeast-dipping fault zones within the Hoh are characterized by intensely deformed mud matrix mélange, and they range from ~200 m to >1,000 m thick; kinematic indicators within the matrix indicate thrusting to the west-southwest. Both hanging-wall and footwall sections are strongly folded and faulted. Wall-rock sections are lithostratigraphically distinct, with hanging walls composed of massive coarse sandstone and conglomerate, and footwall sections composed of thin- to medium-bedded sandstone and siltstone. Folds within the wall-rock sections are oblique to, and are truncated by, the later fault-zone mélanges, indicating that the fault zones postdate folding.

Evidence of fluid involvement in the Hoh rocks includes petroliferous outcrops, carbonate and clay cement, and veins of carbonate and laumontite. The progressive evolution of veins and cements (paragenetic sequence) can be interpreted in terms of crystallization under conditions of increasing consolidation, decreasing salinity, and changing fluid composition. Suppressed carbonate luminescence may reflect crystallization under reducing conditions, perhaps related to the sulfate reduction zone, the presence of hydrocarbons, or clay dehydration. Although deformational features may be associated with the earliest phase of veining, most of the localized grain breakage and matrix shear zones formed after the early micritic veins and before the last phase of sparitic carbonate (+laumontite) veins. Laumontite occurred syn-deformationally and in equilibrium with carbonate, and also post-deformationally.

The paragenetic sequences observed in all samples from the Hoh rock assemblage can be correlated, suggesting that the sources and processes controlling the fluid emplacement were similar across a wide region. In addition, the paragenetic sequence in the Hoh rocks is similar to that documented in autochthonous coeval basins of southwest Washington. This similarity suggests that the precipitates, formed during the evolution of the Hoh rocks, involved fluids that originated within the matrix and did not involve exotic or far-traveled fluids.

INTRODUCTION

Sediments that enter accretionary complexes may initially contain more than 50% water; during accretion this may be reduced to less than 10% by compaction, cementation, and deformation (Bray and Karig, 1985). Thus the process of accretion liberates substantial amounts of pore fluid, which can be augmented by exotic fluids derived both from underthrust sediments (Westbrook and Smith, 1983; Moore, 1989) and devolatilization reactions (Bebout and Barton, 1989; Bebout, 1991; Kastner and others, 1991). In active accretionary complexes, fluid flow may be directly observed using either submersible or drilling studies (Le Pichon and others, 1987; J. C. Moore and others, 1988, 1990, 1991; G. Moore and others, 1990; A. Fisher and Hounslow, 1990; E. Davis and others, 1990). In ancient accretionary prisms, however, fluid migration can only be inferred based upon preserved precipitates (Torrini and others, 1985; Vrolijk and others, 1987; D. Fisher and Byrne, 1990; Speed, 1990).

The Hoh rock assemblage provides an optimal environment to study the vestiges of fluid flow in an accretionary complex, because it ultimately reached only an early stage of deformation and a low grade of metamorphism; it is therefore free of thermal and structural overprinting (unlike the Franciscan [Underwood and others, 1989] and Shimanto [Underwood and others, 1992] complexes). In addition, fluid precipitates are common in the Hoh rocks and can be used to trace the evolution of fluids in the complex. Lastly, previous studies of coeval autochthonous basins in southeast Washington (Galloway, 1974) provide a diagenetic baseline to compare with the Hoh rocks. This comparison provides a basis to determine how much of the fluid history is preserved in the Hoh rocks, as well as the extent of exotic fluid involvement.

The purposes of this paper are to outline the structural history of the Hoh rock assemblage and to tie the fluid precipitates preserved in these rocks to the structural evolution. The structural framework is needed to define the timing and emplacement mechanisms of the fluids, and also to investigate the interaction of fluids and structures. Crosscutting relationships of fluid precipitates and deformational features delineate the paragenetic sequence, whereas the changing composition and character of the fluid precipitates define the chemical and physical environments present during crystallization. By examining the similarities and regional extent of the fluid precipitates preserved in these samples, we address the larger-scale evolution of fluids in accretionary complexes.

GEOLOGIC SETTING AND PREVIOUS WORK

Late Miocene to Pliocene oceanic crust is currently being underthrust beneath coastal

*Present address: Monterey Bay Aquarium Research Institute, 160 Central Avenue, Pacific Grove, California 93950.

Geological Society of America Bulletin, v. 105, p. 1053–1075, 19 figs., August 1993.

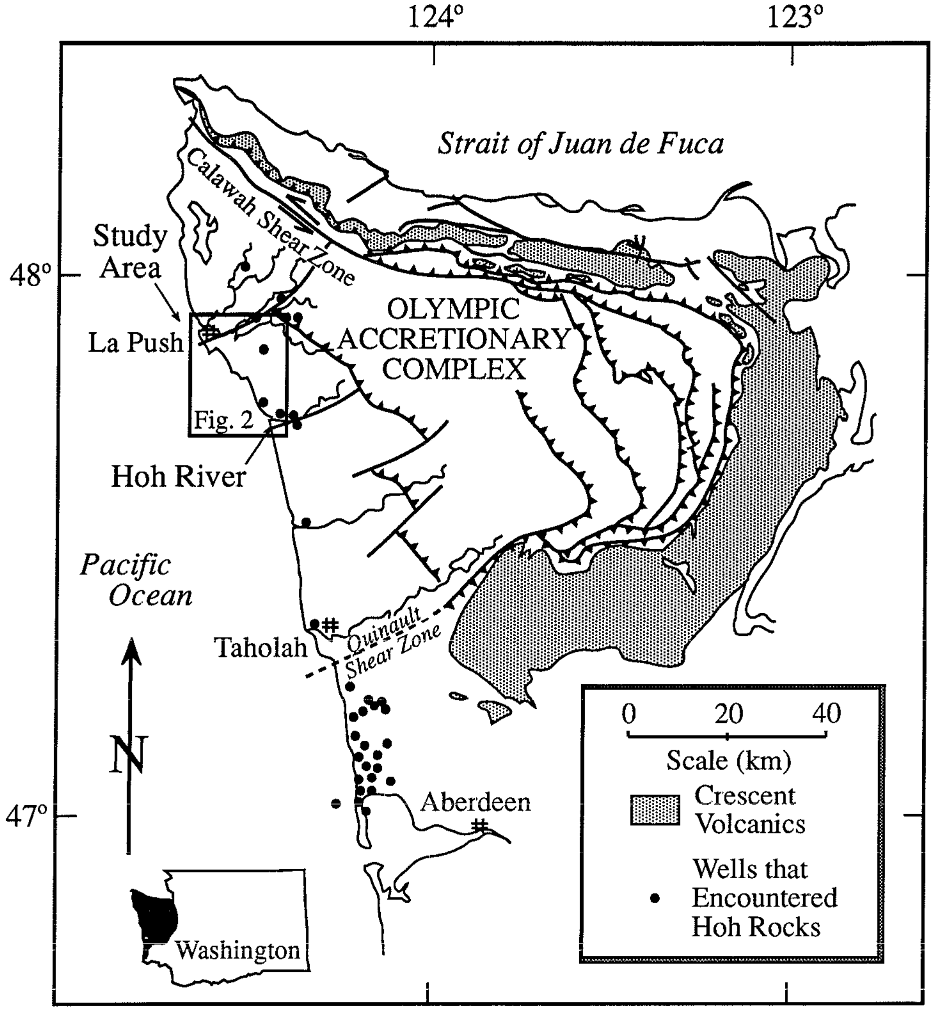

Figure 1. Geology of the Olympic Peninsula, Washington (central and eastern Olympics after Tabor and Cady, 1978b; western Olympic Peninsula after Snavely and Kvenvolden, 1989; Rau, 1979; Stewart, 1970). The Hoh rock assemblage consists of accreted Eocene to Miocene marine sequences that are subaerially exposed between Taholah and La Push.

Washington and Oregon at 3.9 cm/yr along an azimuth of 70° (DeMets and others, 1990; Riddihough, 1977; Engebretson and others, 1985); paleotectonic reconstructions indicate that the adjacent spreading center has been in proximity to the continental margin for the past 30 m.y. (Engebretson and others, 1985). West of Washington, the incoming oceanic crust is covered by at least several kilometers of sediment deposited by prograding submarine fans that filled the trench with predominantly terrigenous sediments (Kulm and others, 1984; Cowan and Potter, 1986). These sediments are quite porous (Kulm, von Huene, and others, 1973) and therefore provide an abundant source of water as they are accreted to the margin and compacted. Seismic images of the region offshore show a complex structural style exhibiting faulting, folding, and mud diapirism (Silver, 1972; Seely, 1977; Snavely and Wagner, 1982; Cowan and Potter, 1986; Wagner and others, 1986). Heat-flow data from offshore Washington (P. Snavely, 1989, personal commun.) and from northwestern Oregon (Blackwell and others, 1982) indicate present-day geothermal gradients of 25–31 °C/km.

The Olympic Peninsula exposes the products of Tertiary accretion in the Cascadia subduction zone (Fig. 1; Stewart, 1970; Rau, 1973; Snavely and Wagner, 1982; Tabor and Cady, 1978a; Cowan and Potter, 1986; Snavely, 1987). In the western Olympic Peninsula, the Hoh rock assemblage (Palmer, 1927; Weaver, 1937; Rau, 1973, 1975, 1979) is composed of Eocene to Miocene sedimentary rocks that occur as broken formation and mélange cropping out along the coast between La Push and Taholah (Fig. 1); maximum metamorphic conditions reach laumontite grade (Stewart, 1974). The intense deformation, scale of fault zones, and mild metamorphism in these units argue for deformation during offscraping or shallow underplating of sedimentary rocks deposited on the abyssal plain (Moore and Sample, 1986). Rau (1979) first interpreted the mélange belts between La Push and the Hoh River as thrust zones, based upon an extension of Stewart's (1970) more detailed mapping south of the Hoh River. In this study, we concur with this interpretation, although we point out that not all of the mélange zones exposed on the western Olympic Peninsula have a thrust origin (Orange, 1990). A fault origin is inferred based upon the intense matrix deformation, consistent matrix orientations, millimeter-scale scaly fabric throughout the mélange zone, and similar orientation of clasts within the mélange (see Orange, 1990). Clasts within these mélange zones are usually massive graywacke sandstone, with less-common graded beds and conglomeratic clasts. Volcanic clasts are rare and consist of massive basalt, pillow basalt, and volcaniclastic breccia.

The pre-Pliocene rocks of the western Olympic Peninsula fall into two depositional age groups, an older one of middle to late Eocene age, and a younger one of late Oligocene to middle Miocene age (Snavely and Kvenvolden, 1989). Based upon these age differences, Snavely and Kvenvolden (1989) referred to these as the Ozette and Hoh mélange and broken formations, respectively. These units, however, are difficult to differentiate in the field. Thrust faults in the coastal exposures of both terranes include Miocene and Eocene microfossils (Fig. 2). There is also no regular pattern of microfossil ages in hanging-wall and footwall blocks. In our mapping, we have been unable to differentiate between an Eocene Ozette and a Miocene Hoh terrane in the coastal region based upon age of deposition, age or style of deformation, or tectonostratigraphic divisions; we therefore adhere to the name "Hoh rock assemblage" for the Eocene to Miocene units of the western Olympic Peninsula (Rau, 1973, 1975, 1979).

The highly deformed Eocene to Miocene rocks of the western Olympic Peninsula are unconformably overlain by shallow-water Miocene (?) to Pliocene marine sequences. In the area east of La Push, this unit is termed the "Quillayute Formation" (Reagan, 1909; Rau, 1979) and is composed of friable sandstone, with beds of fossiliferous pebble con-

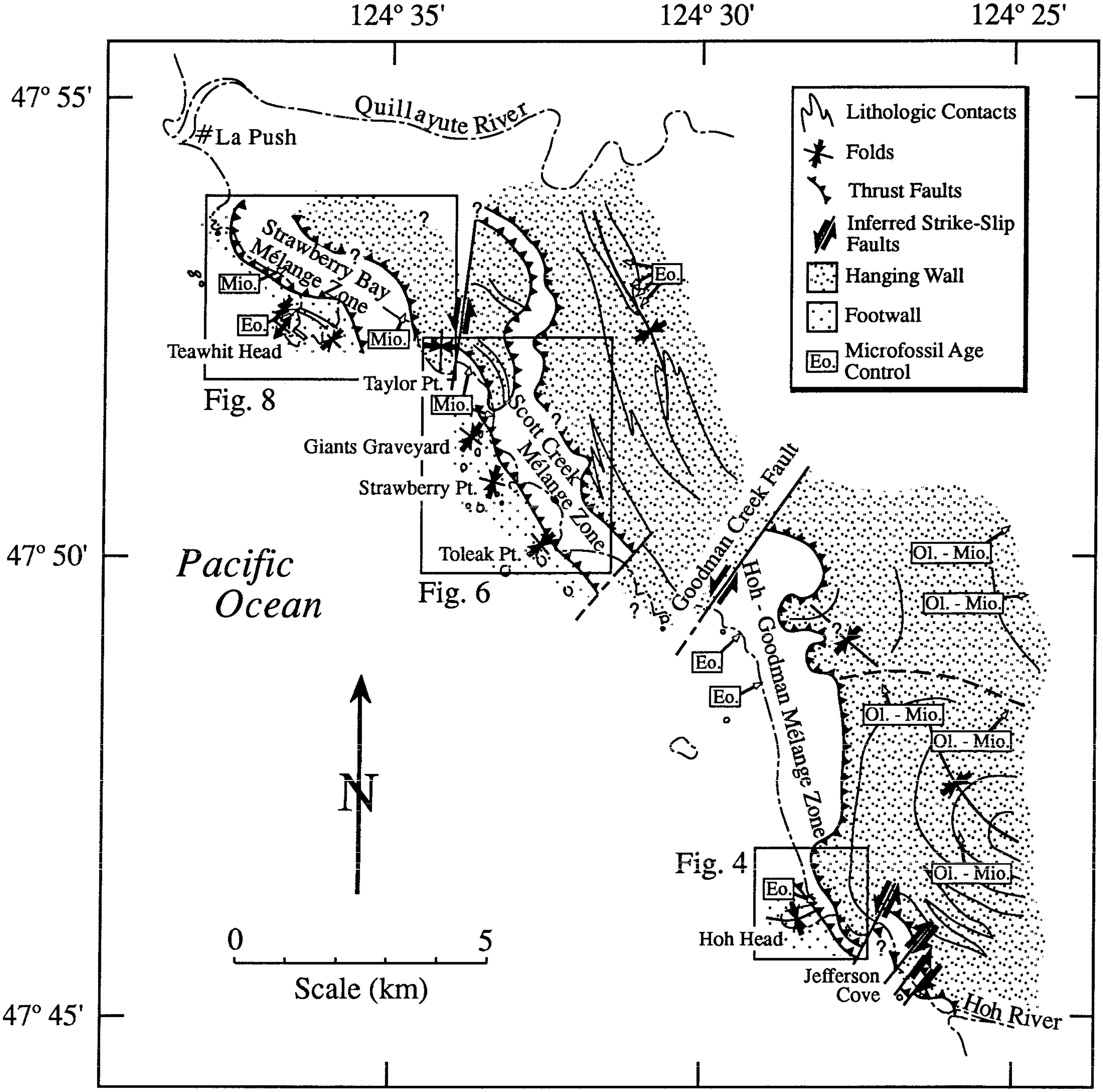

Figure 2. Geologic map of the Hoh rock assemblage between La Push and the Hoh River (after Stewart, 1970; Rau, 1979; Orange, this study; microfossil age dates after Rau, 1979).

glomerate. Maximum dips of 17° attest to its moderate deformation. In the region surrounding Taholah (Fig. 1), a unit of similar age (although possibly slightly younger; Rau, 1979) is termed the "Quinault Formation" (Arnold, 1906; Rau, 1970). The lithology of the Quinault varies from massive sandstone and conglomerate to thinner beds of sandy siltstone, and this unit is also only moderately deformed (dips commonly between 10° and 25°, with some high-angle faulting). Seismic surveys and numerous test wells both offshore and onshore indicate the regional extent and complex deformational style of the pre-Pliocene units as well as the extent of the Quinault and Quillayute (?) Formations and their increased thickness offshore (Snavely and Wagner, 1982; Cowan and Potter, 1986; Wagner and others, 1986; Rau and McFarland, 1982).

Sedimentary strata within the Hoh rock assemblage were deposited between Eocene and late Miocene time, then accreted to the continental margin, deformed, uplifted, and eroded by latest Miocene to Pliocene time.

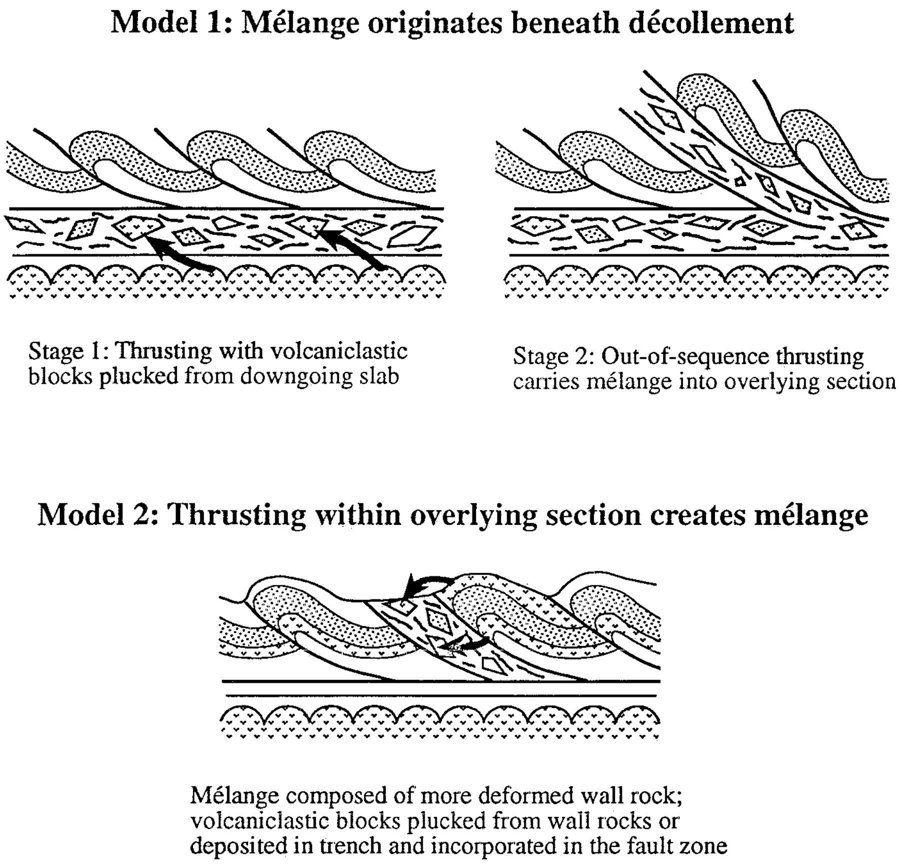

Figure 3. Two models for the origin of thrust-fault mélanges in the Hoh rock assemblage (after T. Byrne, 1992, written commun.).

This rapid and intense deformational history is free of any thermal or strong structural overprint, allowing for the detailed examination of, and the interaction between, the tectonic and fluid histories.

THE HOH ROCK ASSEMBLAGE: STRUCTURAL GEOLOGY AND GEOMORPHOLOGY

Field mapping was conducted at scales ranging from 1:62,500 to 1:10,000. Most maps were assembled at a scale of 1:24,000. Rock units within the hanging walls and footwalls of these fault zones are composed of relatively coherent siliciclastic sections of Eocene to Miocene Hoh rocks (Rau, 1979). Units within the wall rocks are broadly to tightly folded and are faulted as well. We have found that there is a difference between the hanging-wall and footwall rocks along the coastal exposures. In the La Push to Hoh River region, the hanging walls are composed of thickly bedded, massive, coarse sandstone and conglomerate (unit Th_{cs} of Rau, 1979). Footwall rocks, by contrast, consist of interbedded sandstone and siltstone, varying from thick- to thin-bedded (units Th_s and Th_{ss} of Rau, 1979). Although these divisions are largely consistent with the mapping of Stewart (1970) and Rau (1979), our mapping redefines the rock unit at Hoh Head. This tectonostratigraphic framework is critical to the mapping in this project and serves to identify two previously unmapped thrust faults at Hoh River and western Taylor Point (see Fig. 2).

The coast of the western Olympic Peninsula is characterized by a variety of geomorphic features. Where the structural grain is parallel to the coast, the coastline is relatively straight, and excellent exposures of mélange are evident (Orange, 1990). In these regions, the fault-zone–wall-rock contacts are parallel to the coast, and where they are present inland, they are poorly exposed and difficult to map in detail. In contrast, where the structural grain is oblique to the trend of the coastline, resistive hanging-wall and footwall sections form prominent headlands, whereas erosive fault-zone mélanges form coves. This latter geomorphic style is present in the study area between La Push and the Hoh River (Fig. 2) and results in high-quality exposures of complete hanging-wall–fault-zone–footwall sections. Three high-angle faults, inferred as strike-slip by Rau (1979), divide the field area into distinct structural blocks.

In the present study, we have focused on three mélange zones exposed between La Push and the Hoh River. From north to south, these are, respectively, the Strawberry Bay mélange zone, Scott Creek mélange zone, and Hoh-Goodman mélange zone (Fig. 2; nomenclature after Rau, 1979). The purpose of this study was to examine the deformation and fluid events related to the development of the accretionary complex; we have thus avoided the northeast-striking, high-angle faults present in the field area, which have restricted zones of deformation associated with them.

Mud-matrix mélange may originate as a diapir, olistostrome, or fault zone. The three mélange zones located between La Push and the Hoh River were originally mapped as thrust faults by Rau (1979) and Stewart (1970). Although we share this interpretation, we point out that it does not address whether or not the fault zones are exotic to the wall rocks. The mélange may originate as a thrust décollement below a sequence of rocks, with incorporation into the section by later out-of-sequence thrusting (model 1, Fig. 3). Alternatively, the mélange may form *in situ* by progressive faulting and deformation of the wall rocks (model 2, Fig. 3). On the western Olympic Peninsula, most of the clasts are lithologically similar to the wall rocks, and the few depositional ages obtained from the mélange (unspecified for matrix or clasts) match the ages of the wall rocks. These observations support model 2. The presence of rare volcaniclastic clasts, however, supports model 1, because interbedded volcanic units are not identified in this region of the Olympic Peninsula. In model 1, volcaniclastic clasts could represent plucked-off parts of the downgoing slab. To be consistent with model 2, these clasts could have originated as detrital blocks deposited in a trench or fore-arc basin or as interbedded volcanic rocks in the accreted section such as those exposed elsewhere on the Olympic Peninsula (Tabor and Cady, 1978a, 1978b; Snavely and Kvenvolden, 1989). If the mélange is exotic to the present-day wall rocks, then its fluid and thermal history may be entirely different; if the fault zones are out of sequence, then the hanging-wall rocks may have a history different from that of the foot wall.

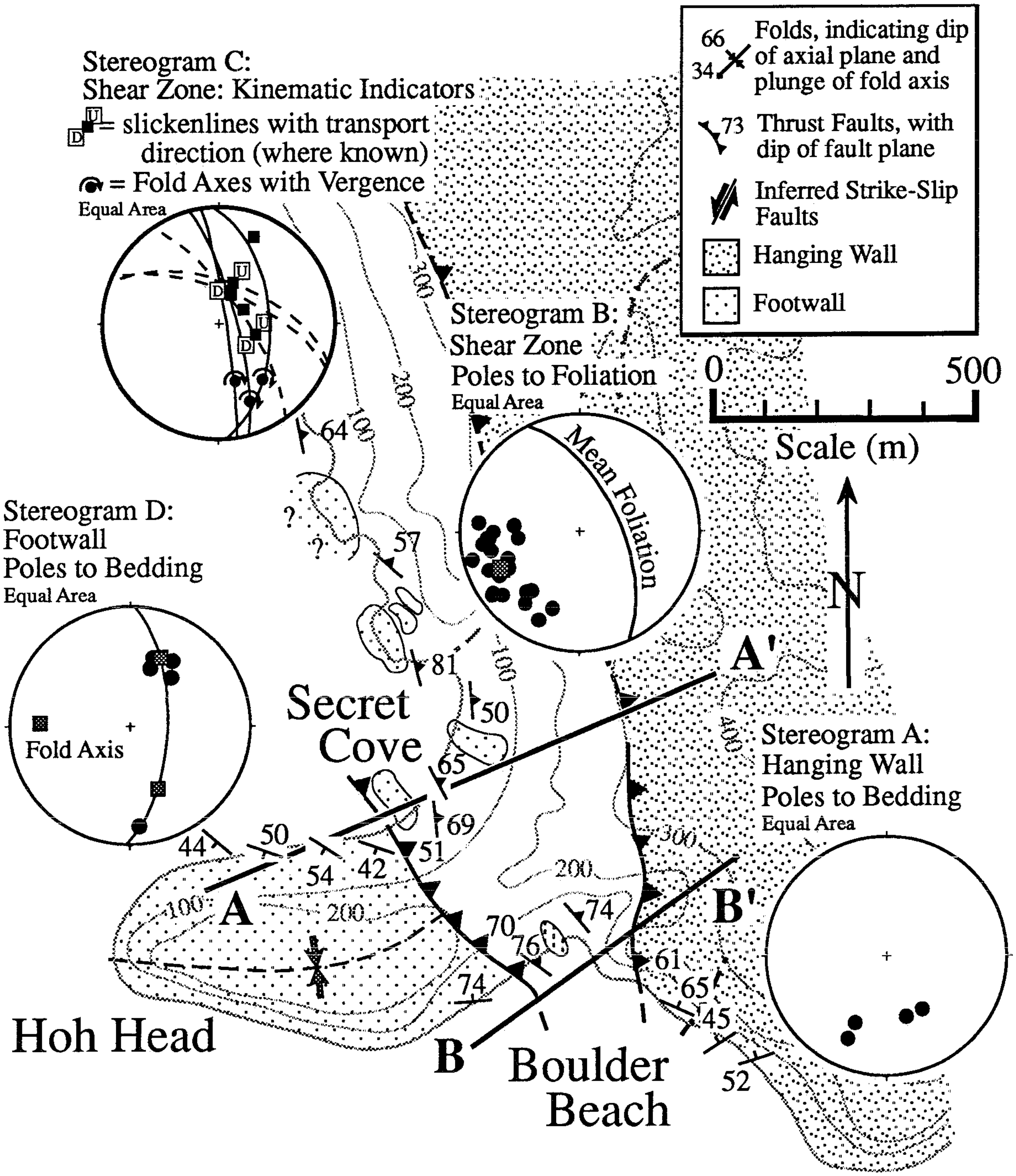

Figure 4. Detailed geology of the Hoh Head region (elevation in feet). Note the complete hanging-wall–fault-zone–footwall sections visible on both sides of Hoh Head. The Hoh Head syncline is truncated by the fault zone, indicating that the fault zone is out-of-sequence.

Field Observations

Hoh Head. Hoh Head provides one of the best exposures of continuous outcrop from footwall to fault-zone mélange to hanging wall (Fig. 4). Complete sections are visible on both the north and south sides of Hoh Head. The hanging wall at Hoh Head ("Mosquito Creek Anticline" of Rau, 1979) is composed of massive to thickly bedded sandstone and conglomerate. Siltstone is absent in this unit. Microfossils indicate deposition from Oligocene to Miocene time (Rau, 1979). The hanging-wall unit is best exposed on the south side of Hoh Head, and bedding orientations indicate a moderate to steep north dip (stereogram A, Fig. 4). Small faults in this section preclude defining a fold axis, although Rau's (1979) mapping suggests a syncline that plunges steeply to the east. The contact between the hanging wall and the mélange zone strikes north and dips steeply, varying from vertical to 60° east. On the north side of Hoh Head, the hanging wall forms a distinctive geomorphic ridge at a height of 100 m; isolated outcrops confirm the hanging-wall rock types of massive sandstone and conglomer-

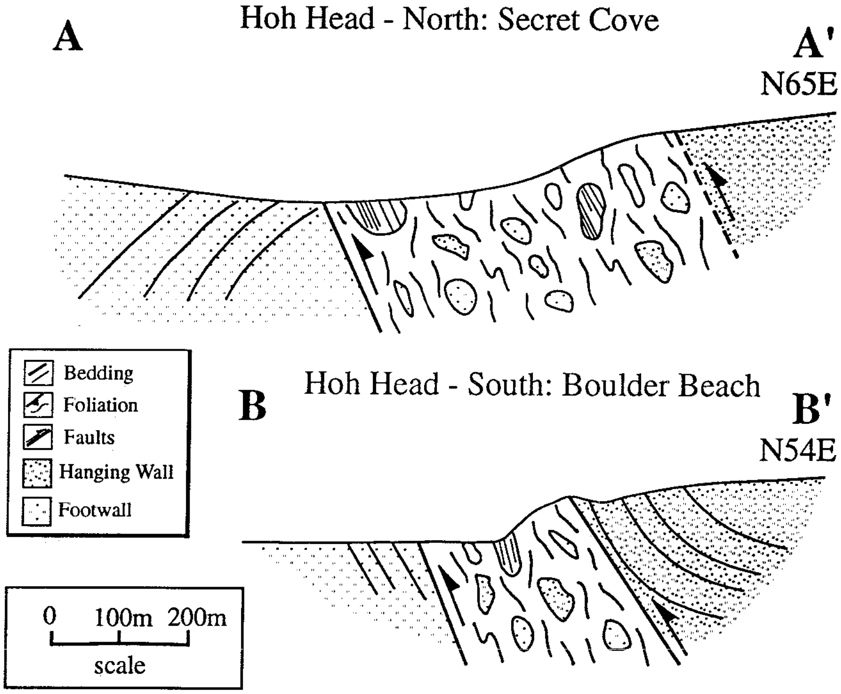

Figure 5. Cross sections in the vicinity of Hoh Head (no vertical exaggeration). Both the hanging wall and footwall are characterized by folding that is truncated by the fault zone, whereas the foliation within the fault zone is consistent in orientation throughout the exposure.

indicated uniform north-northwest strikes and steep dips to the east.

The shear-zone mélange is visible in tidal and beach-front exposures throughout this region; exposure ranges from poor to excellent, with the better exposures indicated by the higher density of foliation attitudes (Fig. 6). The foliation within the mélange is characterized by a pervasive millimeter-scale, scaly fabric that is relatively uniform in intensity throughout the mélange. From south of Toleak Point to Scotts Bluff, this foliation strikes north-northwest and dips moderately to steeply to the northeast (stereogram A, Fig. 6). Given a mean dip of 60° for the mélange and the position of the hanging wall, this fault zone is ~1,000 m thick at Toleak Point (Fig. 7), although this thickness may increase substantially to the north. Microfossils from one locality within the fault zone (unknown whether block or matrix, Fig. 2) indicate a Miocene age (Rau, 1979). Southeast-plunging folds in the mélange matrix show clockwise vergence, whereas the northwest-plunging fold has a counterclockwise vergence (stereogram B, Fig. 6). These attitudes define a separation arc indicating thrusting to the west-southwest (Hansen, 1971).

Matrix foliation orientations between Scotts Bluff and Taylor Point are less consistent (Fig. 6). The attitude at Scotts Bluff clearly may be related to wrapping around the adjacent wall rock, whereas at Taylor Point, the matrix may be affected by the nearby high-angle fault. Unfortunately, much of this cove was slumped, and good matrix outcrops were rare.

At Scotts Bluff, the fault zone appears to bifurcate, with matrix mélange outcrops visible in the Scotts Creek valley to the east and in the low-tide exposures to the west. The Scotts Bluff section is composed of interbedded massive sandstone with some conglomerate, and appears to be of "hanging-wall" affinity. Given the lack of inland outcrop and the juxtaposition of a high-angle fault just to the west, it is difficult to discern whether Scotts Bluff is a megablock within a larger fault zone, or whether this signifies a lateral branching of the fault zone. Neither interpretation can be ruled out.

The footwall of the Toleak Point–Strawberry Point–Giants Graveyard section is composed of thin- to medium-bedded graywacke sandstone and siltstone. These units are variably deformed, ranging from open to tight folds at Toleak Point to tight folds and closely spaced faults at Giants Graveyard and Strawberry Point (Fig. 7). Axial surfaces of

ate, yet the massive aspect of these units precludes accurate determinations of bedding attitudes.

The fault-zone mélange exposed at Hoh Head has a consistent orientation throughout the extent of its outcrop, from Boulder Beach to the Goodman Creek fault zone to the north over a total distance of 7 km along strike. The matrix foliation strikes to the north-northwest and dips steeply to moderately to the northeast (stereogram B, Fig. 4). On Hoh Head, the mélange zone forms a distinct saddle between the more resistant hanging-wall and footwall rocks (see Fig. 31 in Rau, 1980); this geomorphic expression is consistent throughout the field area. Age control of the mélange (unknown whether blocks or matrix) comes from Eocene microfossil localities at Hoh Head and just south of Mosquito Creek (Rau, 1979).

Slickenlines associated with hanging-wall and footwall contacts, as well as asymmetric folds in the mélange matrix, indicate east-side-up thrust vergence (stereogram C, Fig. 4). In cross section, the Hoh Head fault-zone mélange varies from 200 m thick on the south to 500 m thick on the north (Fig. 5). The contact between the fault zone and the footwall is well exposed on both the north and south sides of Hoh Head, and dips from 51° to 70° to the northeast. The contact is at high angles to the bedding in the footwall (Fig. 5) and is characterized by severely disrupted footwall rocks intermixed with the fault-zone matrix mélange. Bedding dips within the footwall range from moderate and south-southwest on the north to steep and north on the south. The Hoh Head footwall syncline (Rau, 1979) has a steep, east-west–trending, axial surface and a shallow, west-plunging, fold axis (stereogram D, Fig. 4). Note that the adjacent fault zone mélange is not folded, indicating that the folding of the footwall occurred prior to faulting. The fault-zone mélange is therefore out of sequence, in that it postdates and is noncoaxial with the deformation in the footwall.

Toleak Point–Strawberry Point–Giants Graveyard. The hanging wall in the region between Toleak Point and Giants Graveyard is identified based upon the presence of a distinct topographic ridge, scattered outcrops of massive sandstone and conglomerate in the creeks southeast of Toleak Point, and published mapping on the logging roads to the east (Fig. 6). Fossils from one locality within the hanging wall ("Murphy Creek Structural Block" of Rau, 1979) indicate an Eocene depositional age (Fig. 2). The massive outcrops and poor exposure precluded determination of bedding attitudes in the hanging wall, although the regional mapping of Rau (1979)

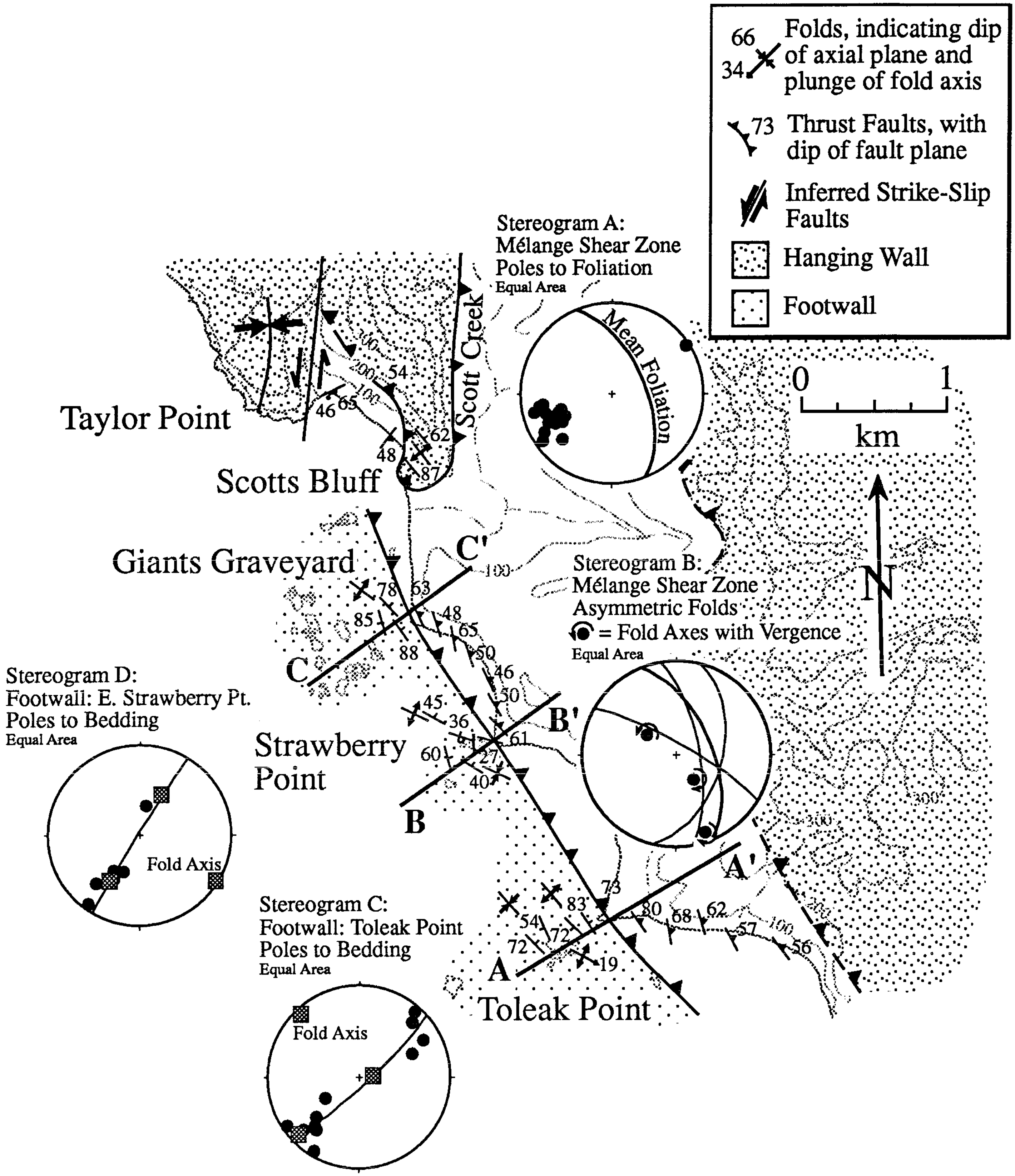

Figure 6. Detailed geologic map of the Toleak Point–Strawberry Point–Giants Graveyard region (elevation in feet). Hanging-wall contact based on Stewart's (1970) and Rau's (1979) mapping, creek traverses, and geomorphology. Matrix mélange crops out on both sides of Scotts Bluff, implying that it is either a megaphacoid within the mélange or a region where the fault zone branches laterally.

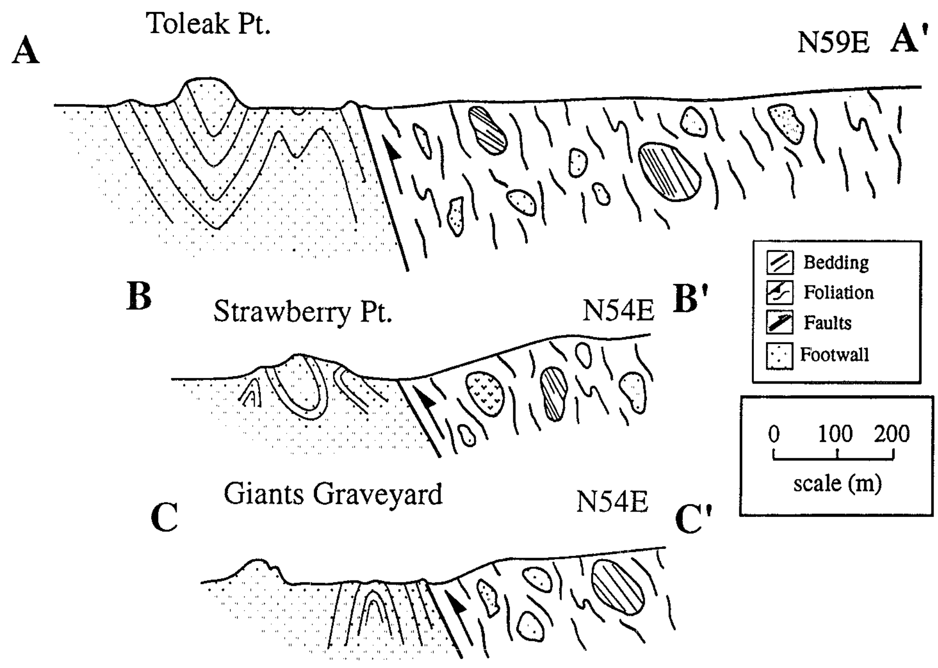

Figure 7. Cross sections through the Scotts Creek mélange zone and associated footwall sections (no vertical exaggeration). The location of the hanging wall is off the scale of the sections shown, 1.2 km (Toleak) to >3 km (Giants) northeast of the footwall–fault-zone contact. An approximate thickness of the fault zone at Toleak Point is 1,000 m.

these folds tend to be steep with north-northwest strikes, whereas fold axes dip shallowly to the northwest or southeast (Toleak Point: stereogram C; Strawberry Point: stereogram D; Fig. 6). Although several of these folds may be related to the main phase of faulting (for example, Toleak Point), many are oblique to, and apparently cut by, the footwall–fault-zone contact. There is no age control for this footwall section.

Teawhit Head–Second/Third Beach–Taylor Point. The contact between Taylor Point and Third Beach was previously mapped by Rau (1979) as a right-slip fault striking N40°E. Where present, this contact is steep to vertical, strikes N20°W to N5°W, and juxtaposes massive sandstone and conglomerate of Taylor Point with the erosive mud matrix mélange of Third Beach (Fig. 8). In addition, there is a geomorphic bench along this trend to the northwest. Based upon the stratigraphy of Taylor Point, the geomorphology, and the similarity between the contact orientation and the foliation within the fault-zone mélange, we have reinterpreted the Taylor Point–Third Beach contact as a thrust fault, with Taylor Point in the hanging wall.

Taylor Point can be mapped at only the lowest tides, and bedding orientations indicate that this headland is composed of a syncline. The fold axis of this syncline plunges shallowly to the northeast (stereogram A, Fig. 8), and although not well defined, the axial surface strikes north with a steep east dip. The oblique trend of the Taylor Point fold and the lack of folding in the mélange indicate that this fold predates the thrust faulting.

The Second and Third Beach fault-zone mélanges are characterized by closely spaced, scaly foliation that is intense throughout the mélange. Foliations within the fault zone strike north to northwest and dip moderately to steeply to the east (stereogram B, Fig. 8). Given the overall dip of the foliation, the Third Beach fault zone is ~600 to 800 m thick (Fig. 9). Two microfossil localities within the Second and Third Beach fault zones (unknown whether block or matrix) indicate deposition in Miocene time (Rau, 1979).

The footwall–fault-zone contact is well exposed on both Second and Third Beaches. The contact dips from 62° to 69° to the northeast, and slickenlines at the Third Beach contact indicate thrusting to the south-southwest (Figs. 8, 10). Asymmetric folds within the Third Beach fault-zone mélange all have moderate to shallow, north-plunging fold axes with counterclockwise vergence, suggesting a northeast-side-up sense of shear (stereogram C, Fig. 8).

The Teawhit Head footwall section is composed of interbedded sandstone and siltstone, with the siltstone-rich sections forming the small coves on this headland. A single microfossil locality on the north side of Teawhit Head suggests that deposition occurred in late Eocene time (Rau, 1979). The Teawhit Head section contains folds, faults, and vein zones of a variety of orientations (Fig. 10). A number of small thrust faults appear to be early features that accommodated bedding-parallel shortening. Normal faults that cut this section are less easy to interpret. In addition to the faults, west-northwest–trending, open-to-tight folds are also encountered; at the Teawhit Head–Third Beach contact, graded beds and cross-stratification indicate that the strata within the footwall have been overturned. A compilation of bedding attitudes from Teawhit Head indicate a fold axis that is near-horizontal and trends northwest (stereogram G, Fig. 10). Based upon the orientation of these folds and the associated pervasive deformation in the axial planar region, we infer that this folding may be related to the Second/Third Beach fault zone mélange.

The mélange fault zone is in contact with a coherent section of interbedded sandstone and siltstone at the northwestern end of Second Beach (Fig. 8). In contrast to the other thrust contacts, this contact strikes northeast and dips steeply to the southeast. Slickenlines on the contact indicate east-side-up, thrust vergence. Unfortunately there are few good matrix outcrops in this area, and so it is impossible to discern whether the foliation is truncated by, or parallel to, this contact. The coherent units are tightly folded about axial surfaces that are parallel to this contact, and fold axes plunge shallowly to moderately to the west. These folds may be related to the adjacent faulting. Rau (1979) suggested that the change in fault-zone orientation is related to the nearby La Push fault. Although our mapping has delineated some of the structural features of this location, the anomalous orientations and uncertain deformational history precluded a more detailed study of fluid precipitates in this region.

Structural Geology: Summary and Discussion

The Hoh rock assemblage of the western Olympic Peninsula is characterized by relatively coherent wall-rock sections and thick fault-zone mélanges. Folds within the wall rocks are oblique to, and are truncated by, the fault zones. The fault-zone foliation is un-

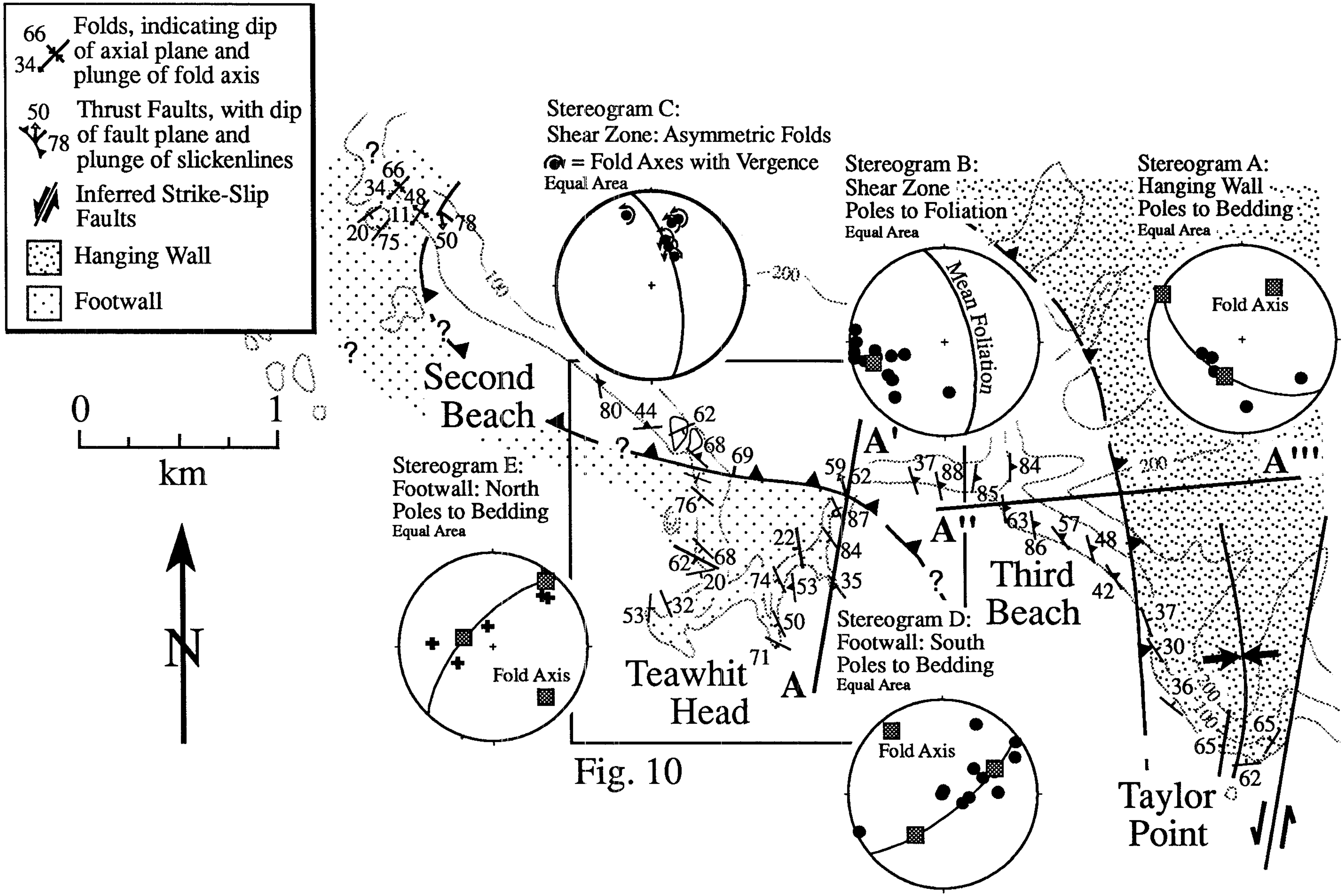

Figure 8. Detailed geology of Teawhit Head–Second/Third Beach–Taylor Point (elevation in feet). The west Taylor Point fault has been reinterpreted in this study as a thrust fault based upon its orientation, regional tectonostratigraphy, and geomorphology.

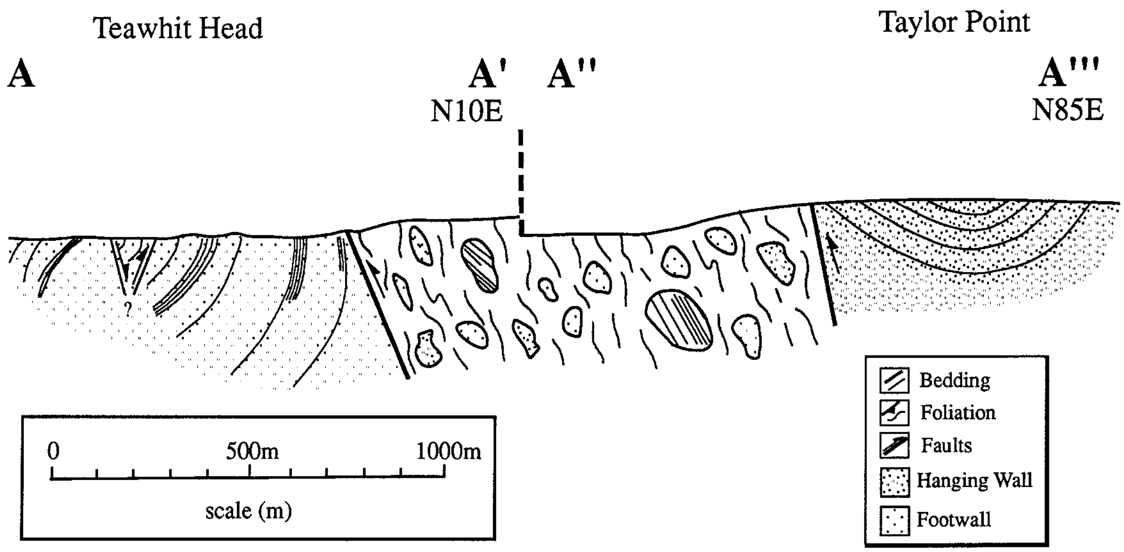

Figure 9. Cross section from Teawhit Head to Taylor Point across the Third Beach mélange zone (no vertical exaggeration). Note the change in orientation needed to plot section perpendicular to wall-rock contacts.

affected by these folds, further indicating that the faulting postdated folding. These fault-zone mélanges, therefore, record "out-of-sequence" displacements. Throughout the field area, the fault-zone foliation strikes north-northwest and dips moderately to steeply to the east-northeast. The mean foliations for the three fault zones are very consistent: Hoh Head (Hoh-Goodman mélange zone) 335/62E, Toleak Point–Strawberry Point (Scotts Creek mélange zone) 337/58E, and Second/Third Beach (Strawberry Bay mélange zone) 346/58E. The mean foliation (all data) for all three fault zones is 339/60E. Because all fault zones have similar orientations and wall rocks, and the high-angle, northeast-striking faults impart minimal deformation on the thrust-fault matrix fabric, we have assembled the kinematic indicators for all three structural blocks (Fig. 11). The mean foliation for the field area is shown, and a compilation of the asymmetric folds shows a clear separation arc indicating west-directed thrusting. The slickenlines at the Hoh Head footwall-fault zone contact are consistent with this interpretation.

The single phase of west-directed thrusting indicated in this study contradicts the two phases of east- and west-directed thrusting suggested by Snavely and Kvenvolden (1989) for the Ozette and Hoh terranes in this area. Our study requires only one phase of pre-Pliocene faulting in the mélange, and we find no evidence of east-directed thrusting in the mélange fault zones.

FLUIDS AND PRECIPITATES IN THE HOH ROCK ASSEMBLAGE

Petroliferous Samples

Field observations in the Hoh rock assemblage indicate abundant fluid involvement in many parts of the complex. "Smell muds," petroliferous matrix mélange materials, are common in many of the mélange fault zones on the western Olympic Peninsula (Lupton, 1914; Rau, 1979; Kvenvolden and others, 1989). Kvenvolden and others (1989) examined samples from widely separated smell-mud localities and found similar molecular marker signatures in all samples, suggesting a common source. Petroliferous samples emit a kerosene-like odor when freshly exposed, ranging from very weak to strong. Petroliferous outcrops include mud-matrix mélange as well as blocks that are entrained within the mélange zones (Fig. 12). The most common petroliferous blocks are graywacke sandstones. No petroliferous sediments or fault zones were detected in the wall rocks.

In addition to petroliferous outcrops, the 50 wells that have penetrated Hoh mélange sections have had oil or gas "shows" (Rau and McFarland, 1982), yet only one has been able to maintain hydrocarbon production at a commercially viable level. The fact that hydrocarbons are associated with mélange fault zones suggests that either these zones are conduits for fluid migration (Snavely and Kvenvolden, 1989), or that the mélange is the source of hydrocarbons. If the mélange were the source of oil, then hydrocarbons could have been concentrated in the shale and mudstone sequences before formation of the mélange. The variability in petroliferous character in clasts in the mélange may be explained either by clasts being exotic to the mélange, or by not being permeable enough to accept hydrocarbons. Alternatively, oil may have migrated from the clasts into the matrix, although if the matrix were overpressured, then this might be against the hydraulic gradient. Lastly, the facts that the fault-zone mélange is petroliferous, and that fault zones within the wall rocks are not, suggest either that the mélange is the source of hydrocarbons, or that the scaly foliation within the matrix acted as both a conduit and a seal against migration into the wall rock.

Veins and Cements

Veins are common throughout the Hoh rock assemblage. These fluid precipitates are abundant in fault-zone sections and include laumontite veins (identified via optical petrography and XRD) and carbonate. Carbonate veins formed throughout the deformational history, whereas laumontite precipitated during and after the last stages of deformation. In the field, laumontite veins may coat scaly foliation surfaces or cut the matrix fabric.

In the wall rocks, the density of veining and the average width of veins increase toward the mélange fault zones. In a number of localities, these veins are along the matrix

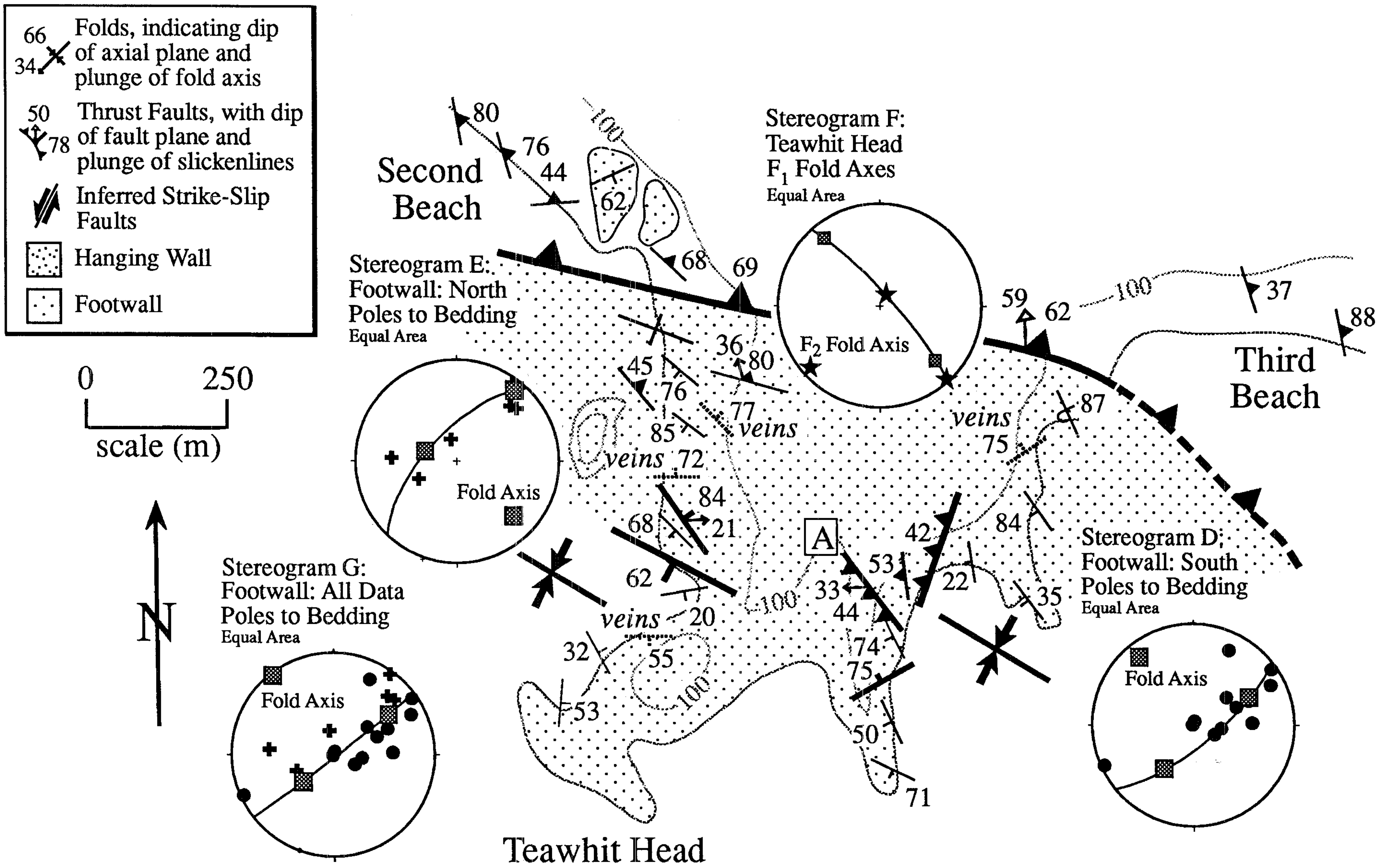

Figure 10. Detailed geologic map of the Teawhit Head footwall. Compilation of bedding data indicate slightly different fold axes for the south and north sides of Teawhit Head (stereograms D, E). This could be due to a broad F2 folding event (stereogram F). The slight difference between these fold axes suggests that deformation on both sides of Teawhit Head is more likely due to a single folding event (stereogram G). Fault zone A is characterized by a pervasive deformational fabric, laumontite veins, and an orientation that is approximately conjugate to the mélange fault zone; a syn-deformational origin is inferred.

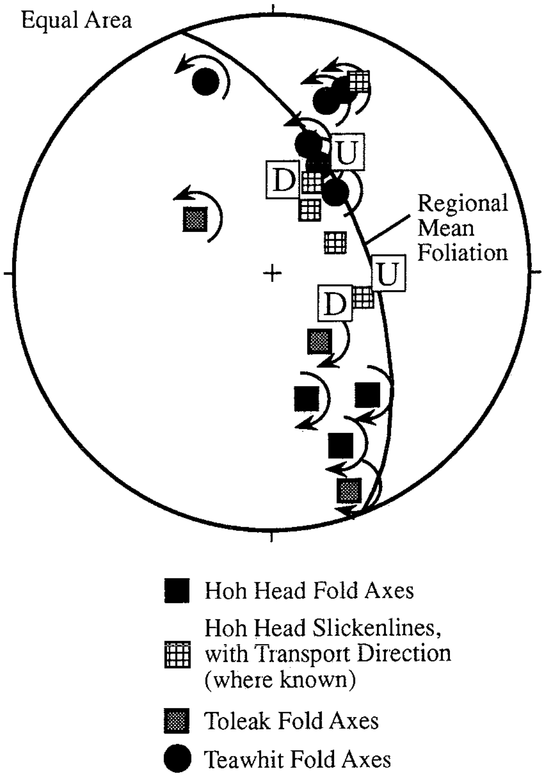

Figure 11. Compilation of kinematic data from the fault-zone mélanges of the Hoh rock assemblage between La Push and Hoh Head. Asymmetric folds and slickenlines indicate thrusting to the west-southwest.

fabric and are continuous from the mélange zone to the adjacent wall rocks. This observation indicates some degree of fluid communication between the fault zone and the wall rocks and could be explained either by fluids flowing from the wall rock into the fault zone, or from the fault zone into the wall rock. In addition, the increase in veining adjacent to the fault zones may reflect an increase in strain magnitude which could lead to a higher degree of wall-rock fracturing and the creation of fluid conduits.

In a related study of the Hoh rocks, Geddes and others (1990) found that the amount of carbonate cement in sandstones increases toward vein zones, from a base level of 3% to as much as 30%–40% adjacent to veins. These elevated concentrations are present as a 10-cm halo around the veins. This association may indicate post-vein compaction of the surrounding rock mass or some degree of fluid interaction between a fracture and its wall rocks. In the latter instance, fluids could be moving from the vein to the wall rock or vice versa, or the cement haloes could be produced by porosity enhancement and calcium diffusion.

Paragenetic Sequence

Given the structural framework outlined above, and the evidence of fluid involvement in all levels of exposure, we now address the fluid history of the Hoh rock assemblage with regard to cementation, deformation, and changing fluid chemistry. Optical and cathodoluminescence observations of precipitates and their crosscutting relationships allow us to assemble a paragenetic sequence (progression of fluid precipitates) for the Hoh rock assemblage (for example, Meyers, 1974, 1978). Nine precipitate and deformation events have been identified for the Hoh rocks, and we use this regional framework for all samples. The paragenetic events for all sections are numbered 1 to 9 (from oldest to youngest).

Techniques. In order to assemble accurate and meaningful data regarding the paragenetic sequence, samples must be examined in the field for the relations between vein and deformation events. In this manner, mesoscopic observations of faulting, discrete cataclastic grain breakage, veins, and cements may be documented. The orientations of veins and structures are also noted.

Vein samples on the scale of tens of centimeters were obtained from fresh outcrops. All samples were slabbed and thin-section–sized targets were selected from these slabs based upon the presence of multiple vein events and/or a clear relation between a fluid precipitate and a deformational feature. Veins cut by deformational features that could be related to the main phase of matrix mélange faulting are termed "pre-deformational," whereas those that cut these features are "post-deformational." If a particular vein event (identified by similar petrographic and cathodoluminescent character) was both cut by and cut a feature related to the main phase of matrix mélange deformation, then it is termed "syn-deformational."

In the following section, the terms "micritic" (<30 μ), "fine spar" (30–80 μ), and "sparitic" (>80 μ) are used to describe the size of carbonate crystals, whereas "dirty" and "clear" are used to describe the clarity of a vein in plane light. "Dirty" veins are those where the presence of included particulate matter results in a dusty appearance under low-power magnification (a function of the number and size of inclusions). The terms "dark," "bright," and the like are used to describe the intensity of carbonate cathodoluminescence (CL). "Distributed" grain breakage refers to isolated examples of grain fracturing, whereas "localized" refers to restricted cataclastic shear zones ("web structure" of Cowan, 1982; Byrne, 1984). "Deformation" refers to faulting, shear fractures and cataclastic grain breakage and not to the fracturing that precedes vein precipitation.

Observations. *Overview.* The overall progression in the Hoh rocks is from an early phase of distributed grain breakage to carbonate cement, localized cataclasis, and a series of carbonate and laumontite veins (Fig. 13). The early carbonate cement is micritic to fine-spar; is present as pore filling and alteration of calcic plagioclase, tuffaceous particles, and Fe-Mg minerals (Koch, 1968); and predates localized cataclastic shear zones (Figs. 13c, 13d). Early cement within the Hoh rocks is indicated by the presence of undeformed mica grains encased within the cement. Retrograded mica grains also lack evidence of alteration-caused wedging open along cleavage. The earliest phase of veining is micritic carbonate with a luminescence similar to the cement (Figs. 13b, 13d, 13e). This first vein commonly contains inclusions of disaggregated grain and matrix, giving it a "dirty" appearance in plane light (Figs. 13c, 13e), and suggesting that the vein formed early in the history. Veins become increasingly sparitic throughout the paragenetic sequence, and the amount of entrained particulate matter also decreases with progressive generations of veins (Figs. 13a, 13c, 13e). Most of the deformation associated with the emplacement of the thrust-fault mélange occurred after the emplacement of the micritic carbonate veins but before the precipitation

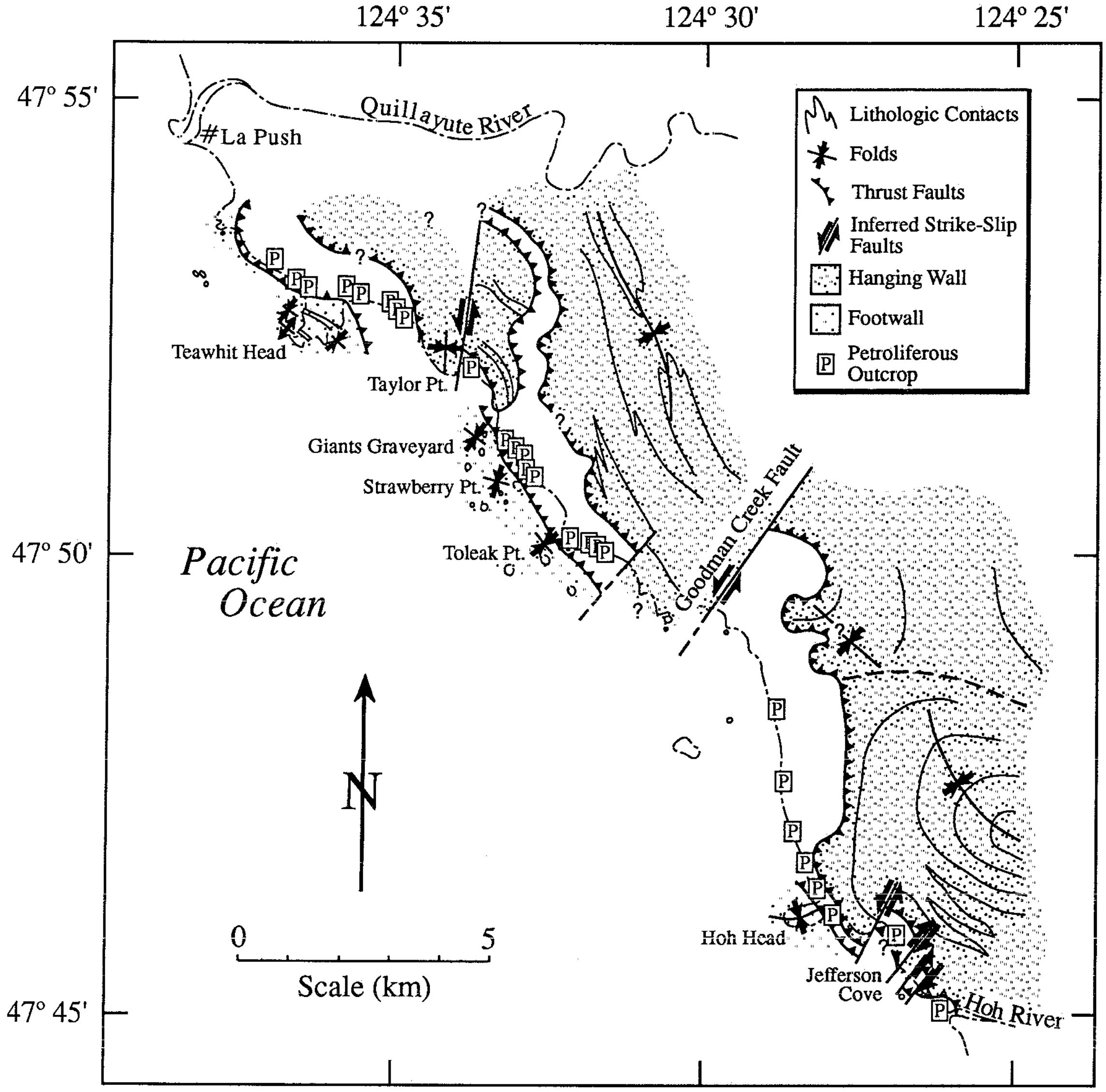

Figure 12. Distribution of petroliferous outcrops between La Push and the Hoh River. Petroliferous samples emit a kerosene-like odor on fresh surfaces and are ubiquitously associated with the northwest-striking thrust faults (Rau, 1979; Kvenvolden and others, 1989; Orange, 1990). No petroliferous sediments or fault zones were found in the wall rocks.

of the bright sparitic carbonate veins (Figs. 13c, 13d). Equilibrium carbonate+laumontite veins formed in the later parts of the paragenetic sequence, and pure laumontite veins characterized the last precipitation event. Other authigenic relationships include clay rinds on some grains, and chlorite replacement of tuffaceous and mafic grains and cement. Grains with clay rinds are found within sparitic carbonate veins, although the timing of clay diagenesis with respect to veining is unclear.

Hoh Head. Samples from both the Hoh head footwall and fault zone demonstrate a similar paragenetic sequence (Fig. 14). Due to the more common observation of cross-cutting veins in the fault-zone samples, more samples were collected from the fault zone ($n = 13$) than the footwall ($n = 2$). Hanging-wall samples lack multiple fluid precipitation events ($n = 5$).

In both the footwall and fault zone, almost all samples contain evidence of abundant early distributed grain breakage (event no. 1; Fig. 14) which is postdated by a micritic, bright cement (no. 2; Figs. 13c, 13d, 13e, 13f). The first vein event is micritic to a very fine spar, has a "dirty" appearance in plane light, and has a luminescence that is identical to the luminescence of the carbonate cement (no. 4 or no. 5; Figs. 13d, 13f).

This early vein commonly forms the margins of veins that were later filled by a darker, sparitic carbonate (no. 6; Figs. 13e, 13f). This gradation indicates a changing fluid composition during precipitation. Zones of cataclastic deformation, as well as discrete fractures, cut these veins in both the footwall and the fault zone (Figs. 13c, 13d). An earlier phase of localized cataclastic shear in the fault zone suggests that deformation began in the fault zones earlier than within the wall rocks.

The final fluid precipitate observed in the footwall is a late, very bright, sparitic carbonate that occurs along irregular dendritic pathways through the samples. This vein event is also present in the fault-zone samples (Figs. 13c, 13d, 13e, 13f), although two of the fault-zone samples have later, syn- to post-deformational laumontite veins that are not observed in the footwall. The syn-deformational veins contain an equilibrium assemblage of laumontite+carbonate (no. 7 or no. 8), and the post-deformational extensional fractures consist of only laumontite (no. 9). In the equilibrium laumontite+carbonate, the carbonate may have the same luminescence as the last carbonate vein.

Toleak Point–Strawberry Point–Giants Graveyard. Both the Toleak Point–Strawberry Point footwall and adjacent fault-zone mélange display similar paragenetic sequences (Fig. 15) with a progression from an early, darkly luminescent carbonate vein to two generations of successively brighter carbonate. In this area, 10 samples were examined in detail from the footwall, and 21 samples were examined from the fault zone. Giants Graveyard and the poorly exposed hanging wall yielded no usable samples.

Most of the samples demonstrate an early phase of distributed grain breakage (no. 1). Within the footwall, nine of the ten samples have an identical precipitate sequence. The earliest precipitate is a dark carbonate cement (no. 2) with a luminescence identical to the first phase of veining. This first vein event is usually dark and micritic, and it is postdated by two brighter, sparitic veins, with the latest vein always brightest in CL. The remaining sample, however, contains a bright cement postdated by a two-phase carbonate vein. The margins of this vein are micritic and bright, with a luminescence similar to the cement, whereas the later core contains a darker, sparitic carbonate. This sample contains a paragenetic sequence similar to that of Hoh Head.

This footwall progression of dark → bright → brighter is consistent with the regional framework, although it can be placed either early or in the middle of the paragenetic sequence (Fig. 15). In these samples, the fact that the earliest, dark carbonate veins are micritic and dirty suggests that they formed early in the history of the rocks (Interpretation 1, Footwall Summary; Fig. 15). Alternatively, if the dark carbonates are correlative, and the micritic or sparitic character a local response, then this vein progression may have formed later in the sequence (Interpretation 2, Footwall Summary; Fig. 15). We favor interpretation 1, based upon the entrained particulate matter in, and micritic aspect of, the early carbonate veins.

The fault-zone samples from the Scotts Creek mélange zone contain a similar progression of fluid precipitates (Fig. 15). Approximately half of the samples demonstrate some distributed grain breakage (no. 1). The oldest vein generation is again a micritic, dark, and optically dirty carbonate (no. 3 or possibly no. 6) which is found either as a narrow vein or as a broader, diffuse vein zone. This vein is postdated by two clear, increasingly bright, sparitic veins (no. 4 and no. 5, or no. 7 and no. 8). Six of the samples contain a syn-deformational, micritic, bright vein that predates a second phase of cataclastic shear as well as darker (no. 6) and brighter, sparitic carbonate veins (no. 7 and no. 8). Lastly, sample DO4 contains an early, dark, sparitic carbonate vein in equilibrium with laumontite (no. 6) that is postdated by two brighter, sparitic carbonate veins (no. 7 and no. 8). Thus, laumontite is not always the last fluid precipitate seen in the Hoh rocks.

As in the footwall, the progression of fluid precipitates observed in the fault-zone samples is consistent with the regional framework, yet it may be interpreted in two ways (Fault Zone Summary; Fig. 15). The progression from dark → bright → brighter can again be either an early (3-4-5) or middle (6-7-8) feature in the overall evolution. The dirty, micritic character of the first vein and its dark luminescence again suggest that it is an early feature (Interpretation 1, Fault Zone Summary; Fig. 15).

Teawhit Head–Second/Third Beach–Taylor Point. Samples from the Second/Third Beach fault zone demonstrate a more protracted fluid evolution than the adjacent Teawhit Head footwall; all are consistent with the regional paragenetic sequence. Five samples were examined from the footwall, twenty from the fault zone. None from the Taylor Point hanging wall contains multiple fluid events and/or crosscutting relationships with deformational fabrics (n = 5).

Most of the footwall samples (DO5, DO6, DO7) came from a 50-m-wide fault zone (fault zone A, Fig. 10) that appears to be conjugate to the larger fault-zone mélange. Several additional samples came from less deformed sections of the footwall. All of these samples present evidence for an early phase of distributed grain breakage (event no. 1, Fig. 16). Three of the samples also display a bright, micritic, early carbonate cement (no. 2) that postdated the grain breakage. The first phase of veining (no. 4 or no. 5) has a luminescence that is identical to that of the cement and consists of a dendritic network of fine sparitic carbonate. This early phase of veining is cut by cataclastic shear zones. Sample DO9 indicates that the next vein event consists of a darker, sparitic to fibrous carbonate (no. 6); in sample DO6, this vein formed syn-deformationally, as indicated by syntaxial fiber growth. This vein is also cut by numerous cataclastic shear zones and a brighter carbonate vein (no. 7 or no. 8); in DO7 this vein contains equilibrium laumontite. Lastly, in three of the five samples (all within the footwall fault zone), the last carbonate vein is postdated by a stage of syn- to post-deformational laumontite (no. 9). Two of these samples contain laumontite precipitating along matrix shears (but undeformed), whereas one of the samples has laumontite both cutting, and being cut by, discrete shear zones. The overall progression in the footwall samples from an early, micritic, bright cement to a later, syntaxial to fibrous, dark carbonate, and then to brighter carbonate and latest laumontite (Footwall Summary; Fig. 16), is consistent among all of the samples. Samples

Figure 13. Plane (A, C, E) and cathodoluminescence (B, D, F) photomicrographs of thin sections from the Hoh rock assemblage that highlight the techniques used for delineating the paragenetic sequence. Scale bar = 0.5 mm. (A, B) Sample DO13, Third Beach mélange zone. Early, moderately luminescent cement is postdated by a vein that progresses from a brighter, micritic margin that is dirty in plane light to a core that is darkly luminescent, sparitic, and clearer in plane light. (C, D) Sample DO15, Hoh-Goodman mélange zone, Hoh Head. The early cement has a luminescence identical to the first vein event, which is a diffuse, micritic carbonate containing abundant particulate matter. This vein is cut by a clearer, sparitic, darkly luminescent calcite, which is cut in turn by a small fault (striking east-west at the bottom of the photo). A sparitic, very clear, brightly luminescent, undeformed vein along this microfault indicates postdeformational precipitation. (E, F) Sample DO16, Hoh-Goodman mélange zone, south of Mosquito Creek. Again, the cement has a bright luminescence similar to the micritic, dirty margins of the vein. The core of this large vein is again filled with the clear, sparitic, darkly luminescent carbonate, whereas the last precipitate is a dendritic network of clear, sparitic, moderately luminescent carbonate (also present in the core of A, B?). The blue luminescent grains in the northeast corner are quartz, and several of these demonstrate early diffuse grain breakage, with the broken grains now isolated in the carbonate cement.

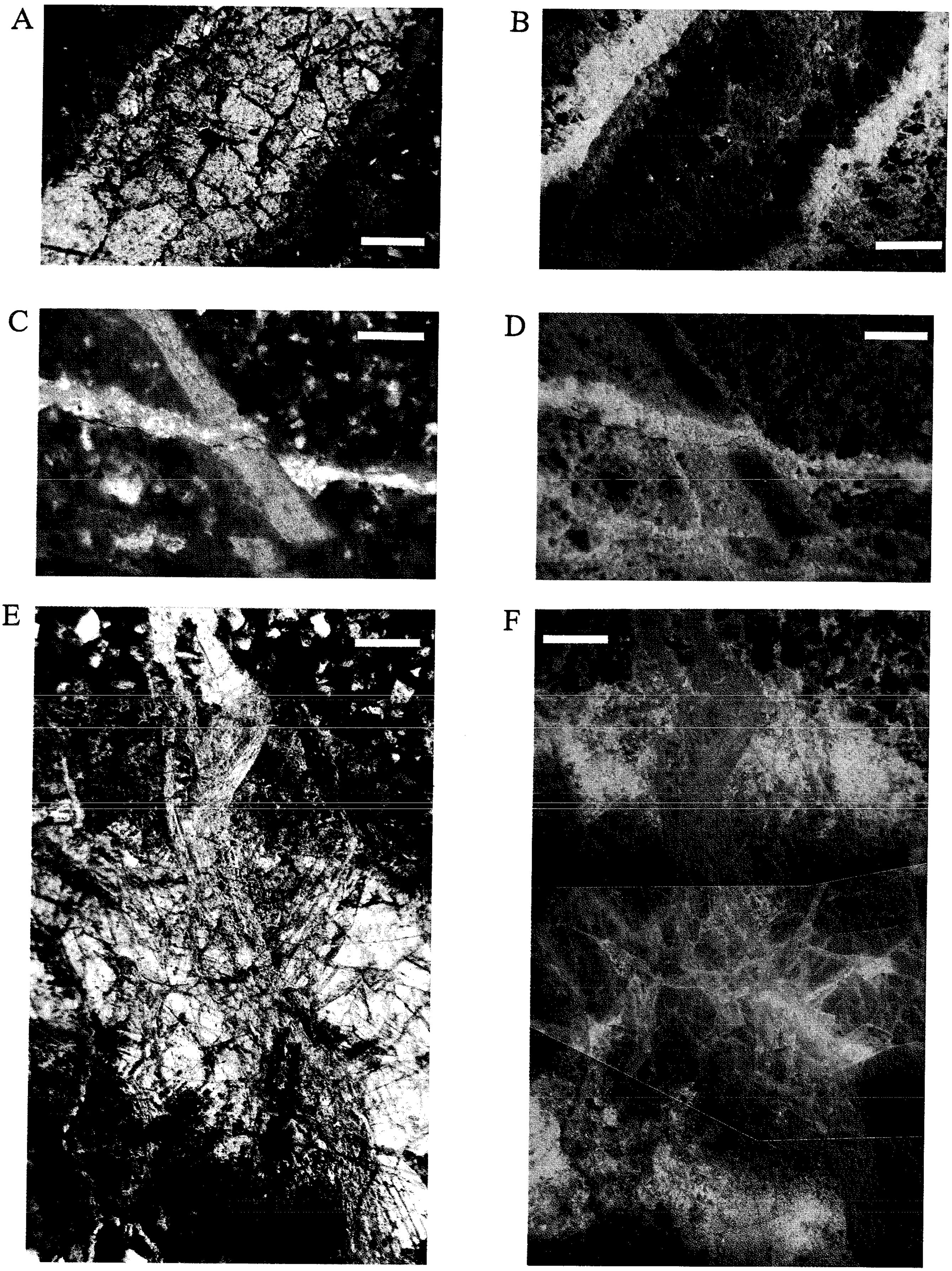
A
B
C
D
E
F

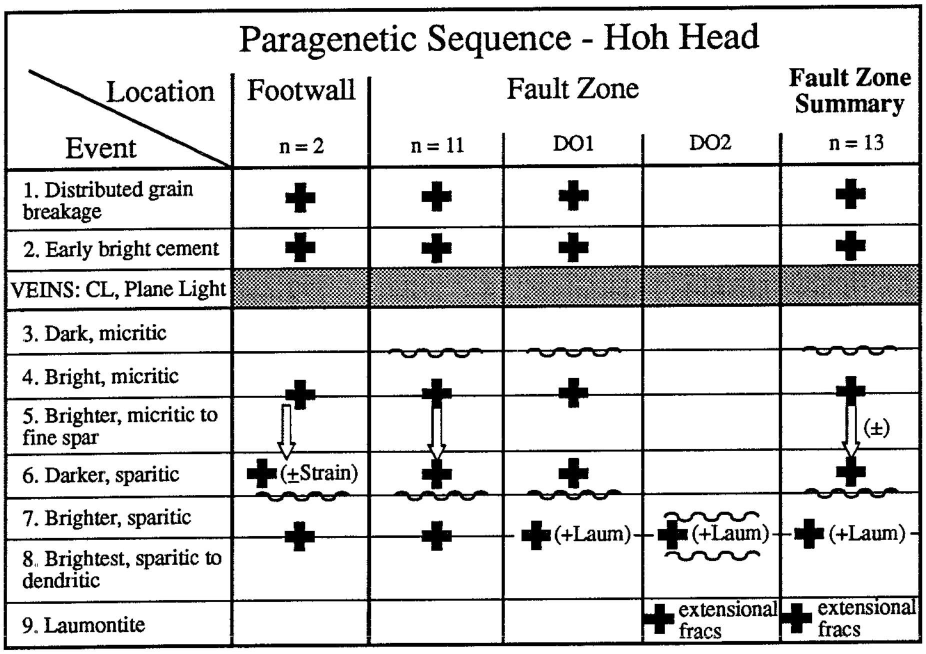

Figure 14. Paragenetic sequence of the Hoh Head footwall and fault zone. Events are listed from older at the top (no. 1) to younger at the bottom (no. 9). "Bright" and "dark" refer to appearance under cathodoluminescence. Crosses signify that a specific paragenetic event is present in this sample. Arrows indicate transitional relations between paragenetic events, with one vein generation occurring along the margins of another vein, for example. Undulating lines indicate discrete faulting and localized cataclastic zones. Where a paragenetic event cannot be correlated with a specific feature, it is shown as either straddling two events or over a range of events. Uncertainties in the presence or timing of precipitates or deformation are indicated by question marks. If a sample has a sequence that is unique, then it has been shown individually; samples with like sequences have been grouped, with the number of such samples shown at the top of the column. Both footwall samples indicate an identical paragenetic sequence, whereas all 15 of the fault-zone samples display a consistent progression.

DO5, DO6, and DO7, from the small thrust-fault zone on Teawhit Head, represent the only occurrence of laumontite in the footwall sections. If this fault zone is in fact related to the main thrust-fault mélange, then there is a diagnostic link between the main phase of thrusting and laumontite precipitation.

In the fault zone, approximately half of the samples contain some distributed grain breakage (no. 1; Fig. 16), and most of the samples have an early, bright, micritic cement (no. 2; Figs. 13a, 13b). Grains in the cement are matrix supported, indicating either higher-than-lithostatic pore pressures and dilation or cement alteration of grain edges during precipitation. In two samples, this early cement is cut by a vein of dark, micritic to fine spar (no. 3), which is in turn cut by a vein of bright micritic to fine spar (no. 4). In all cases, this early, bright vein predates localized cataclastic grain breakage. In ten of the samples, there is a progression from the early, bright micritic vein (no. 4) to a brighter fine sparitic vein (no. 5) and then to a darkly luminescent sparitic vein (no. 6). The dark sparitic carbonate may form the core of two phase veins (Figs. 13a, 13b); may cut the earlier, bright, micritic vein; and usually is cut by localized cataclastic shears. The later, bright, carbonate veins (no. 7, no. 8; diffuse core in Fig. 13b?) are small, sparitic, irregular to dendritic, unstrained along webs, and commonly cut webs and the matrix fabric, suggesting a post-deformational origin.

Several of the Second/Third Beach fault-zone samples also contain various generations of laumontite. Sample DO10 contains an early, large, laumontite vein that is post-dated by cataclastic shear zones; a fine, sparitic, dark carbonate+laumontite vein; and a brighter, sparitic, carbonate vein (Fig. 16). Sample DO12 contains a bright, sparitic, carbonate+laumontite vein and a later, laumontite vein; both contain a large amount of disaggregated grain material, suggesting dilation and fluid-induced brecciation during precipitation. In sample DO11, this brecciated laumontite zone (which in the field reaches >10 cm in width) is cut by localized cataclastic shear zones.

Composite Vein Evolution: Observations and Interpretations. A remarkable aspect of the Hoh rock assemblage samples is that the paragenetic sequences for all samples fall into the same framework (Fig. 17). The overall evolution consists of an early phase of distributed grain breakage (no. 1), followed by an early, bright, micritic cement (no. 2); a dark, diffusive, micritic vein (no. 3, although rare); two generations of bright micritic veins (no. 4, no. 5) that also are observed as micritic to fine, sparitic margins for a later, darker, sparitic vein (no. 6); and then several phases of increasingly bright, sparitic veins (no. 7, no. 8). With the exception of sample DO10 (Third Beach mélange zone), all laumontite veins precipitated with the dark, sparitic carbonate (no. 6), the later, bright, sparitic carbonate (no. 7, no. 8), or after all carbonate precipitation events (no. 9). The main phase of mélange faulting took place after the bright, micritic carbonate (no. 4, 5) but before the precipitation of the bright, dendritic and sparitic carbonate (no. 8) and most of the laumontite (no. 9).

The transition from early, micritic to later, sparitic veins may be due to a number of factors. Classic sedimentary petrology studies attribute this progression to a change in the host fluid chemistry (see Tucker, 1981, p. 135–136; Folk, 1974). In marine bottom-water conditions, early fluids are Mg-rich, and the magnesium selectively inhibits the lateral growth of crystals, leading to the formation of micritic or fibrous magnesian calcite or aragonite with dimensions of less than a few microns (Folk, 1974; Folk and Land, 1975). During burial, the Mg may be removed by dolomitization or clay diagenesis, or lowered by an influx of fresher water; the resulting low Mg/Ca fluid leads to the formation of larger calcite crystals. Thus, the change in the Hoh rocks from micritic to sparitic crystallization could be due to a freshening of the fluid phase. A freshening fluid phase is supported indirectly by the observations of negative chloride anomalies along fault zones in active accretionary complexes (Kastner and others, 1991), and by the increasing freshness of fluids sampled landward from the toe (Vrolijk and others, 1992).

Alternatively, the presence of entrained particulate matter common in these early veins may provide a large number of nucleation sites for crystal formation (Kingery, 1967, p. 297–298). The resultant vein may

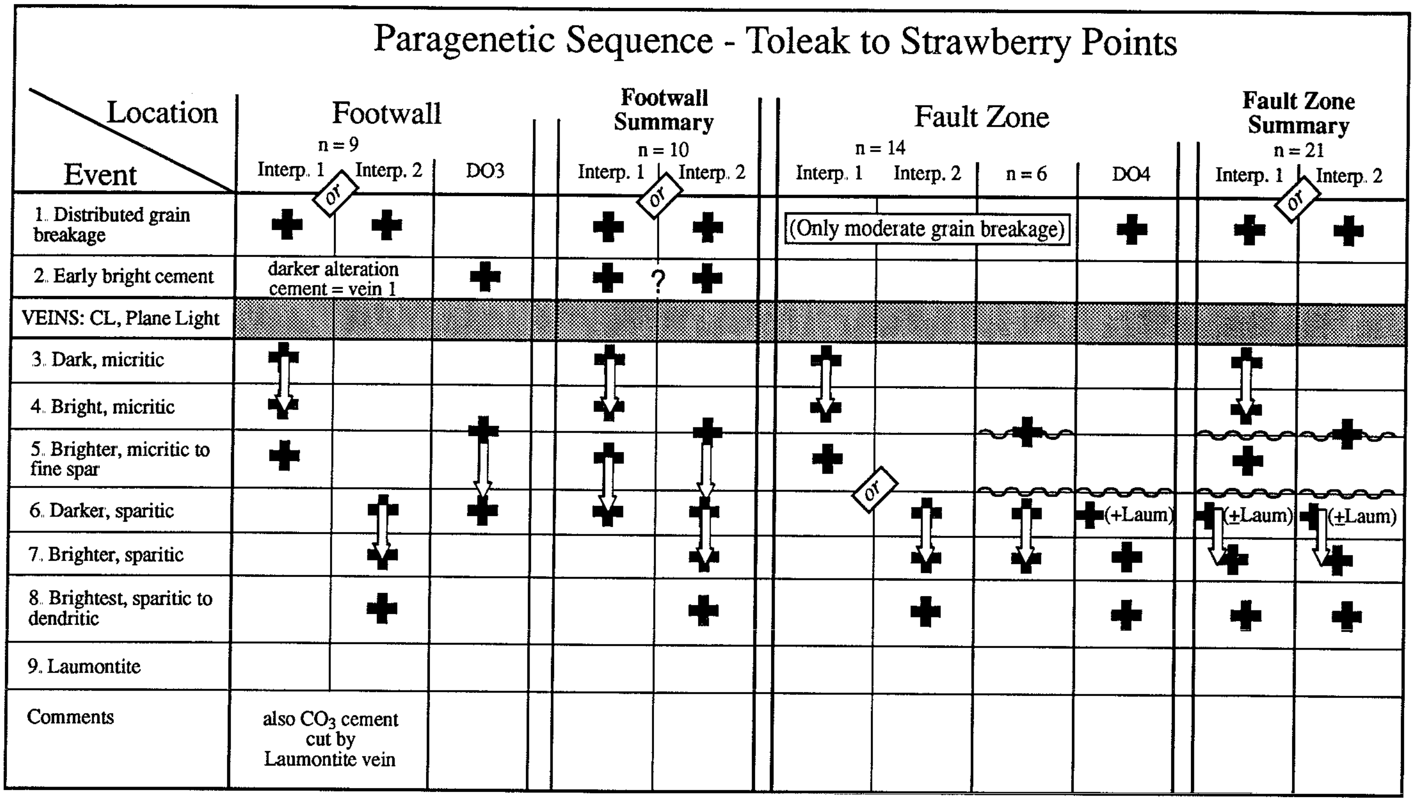

Figure 15. Paragenetic sequence of the Toleak and Strawberry Point footwall sections and the Scotts Creek fault-zone mélange (see Fig. 14 for explanation of symbols). The sequences in both structural domains are consistent with the regional framework, although the dark → bright → brighter progression may be placed in two positions within the sequence. On the basis of the early, darker carbonate appearing dirty in plane light, we favor interpretation 1 for both domains.

have large numbers of very small crystals, giving an overall micritic appearance. In this interpretation, sparitic veins would indicate a higher degree of wall-rock cementation and less entrained matrix within the vein. Further support of this is seen in the rare examples of grain breakage at the margins of some of the sparitic veins (suggesting a high degree of consolidation and a "strong" matrix). Both processes, consolidation and fluid freshening, may have been active during the burial and diagenesis of the Hoh sediments.

The changes in carbonate cathodoluminescence are more difficult to interpret. A wide variety of elements and chemical changes can affect cathodoluminescence (for example, Pb^{+2}, Ce^{+2}, Ni^{+2}, Mn:Fe^{+2}, rare-earth elements, variations in trace-element supply, and clay diagenesis; Machel, 1985). In the autochthonous basins of western Washington, Galloway (1974) observed a second phase of carbonate cement, replacing detrital grains, that coincided with laumontite precipitation and inferred clay dehydration. Thus clay diagenesis (if present in the Hoh rocks) may have affected the carbonate luminescence. We lack data, however, to correlate specific diagenetic features with changes in carbonate luminescence, and none is presented in Galloway. We have therefore based our preliminary interpretation of luminescence changes upon variations in the Mn:Fe^{+2} ratio alone (Tucker, 1981, p. 135). The brightness of carbonate luminescence is strongly affected by the ratio of Mn:Fe^{+2} in the carbonate, with an increase in this ratio leading to an increase in luminescence (Tucker, 1981, p. 135). Preliminary EDS analyses of several samples from the Hoh rock assemblage indicate that brightly luminescent veins have ~3 wt% Mn and ~2.5 wt% Fe (+2 and +3); poorly luminescent veins have less Mn, although there are some variations in this trend.

Further support for the relationship between luminescence and Mn:Fe^{+2} ratio comes from the toe of the modern accretionary complex off Oregon, where samples contain an early bright cement postdated by a darker carbonate cement and vein (J. Sample, 1991, personal commun.). This progression has been interpreted in terms of cementation in the sulfate reduction zone. Reducing conditions lead to an increase in Fe^{+2} at the expense of Fe^{+3} and a subsequent lowering of the Mn:Fe^{+2} ratio. In the Hoh rocks, the earliest micritic, dirty vein is a candidate for precipitation in the sulfate reduction zone, because the entrainment of matrix particulate matter suggests that this vein formed early in the diagenetic evolution prior to significant consolidation and lithification.

Progressively brighter carbonate luminescence could signify less reducing conditions during burial and diagenesis, yet this trend was interrupted by the regional precipitation of the dark sparitic carbonate vein. The suppressed luminescence in this vein may be due to precipitation under reducing conditions related to the onset of hydrocarbon migration; dark luminescence in the presence of hydrocarbons has been documented elsewhere by Barker and Dalziel (1991). The darkly luminescent, sparitic carbonate vein contains the earliest primary petroleum fluid inclusions in the paragenetic sequence (Orange and others, 1990), and yet successive generations of bright sparitic veins also contain primary petroleum inclusions. The dark sparitic vein

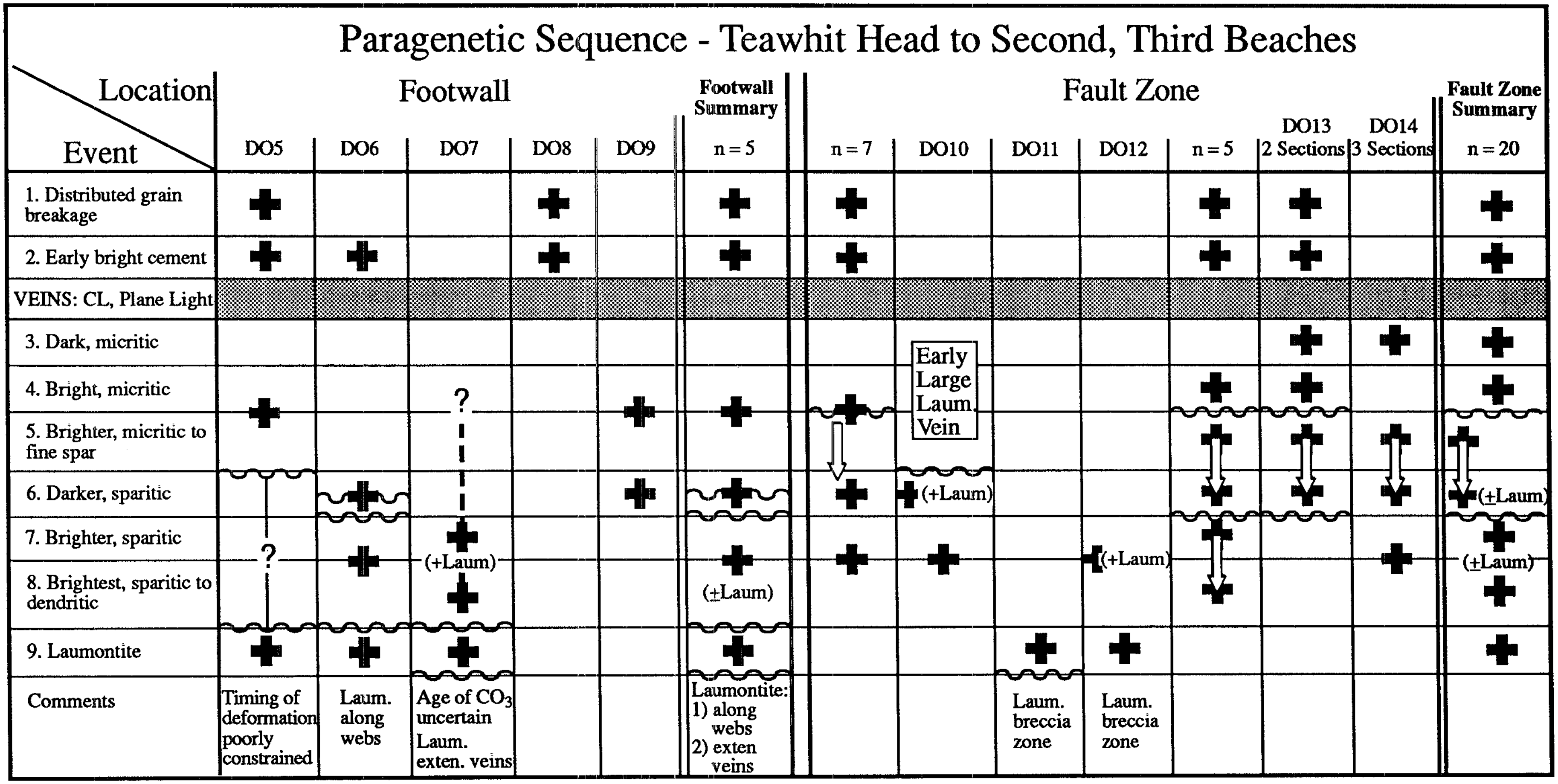

Figure 16. Paragenetic sequence of the Teawhit Head footwall and Second, Third Beach mélange fault zones (see Fig. 14 for explanation of symbols). Note the presence of laumontite in these samples either in equilibrium with carbonate or as a late-stage, post-deformational vein.

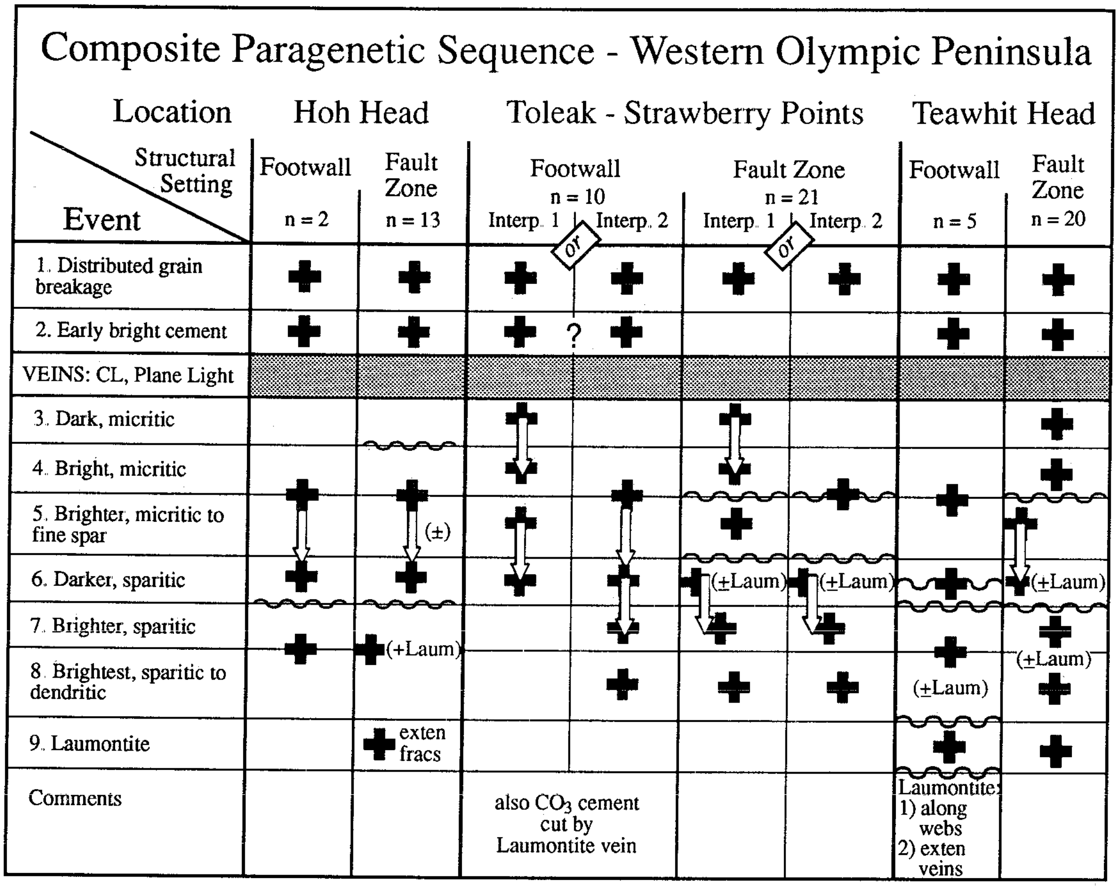

Figure 17. Composite paragenetic sequence of the Hoh rock assemblage, western Olympic Peninsula, containing the integrated sequences for the footwall and fault-zone sections from each of the three structural blocks (see Fig. 14 for explanation of symbols). Despite the large along-strike distance (~30 km), diverse fossil ages (Eocene to Miocene), and disparate structural positions, the paragenetic sequences of all localities are consistent. In addition, the relative timing of the main phase of thrusting can be restricted to have occurred after the precipitation of the micritic carbonate veins (nos. 3, 4) and before the precipitation of the bright, sparitic carbonate (nos. 7, 8) and laumontite (no. 9).

may indicate the onset (and peak?) of petroleum migration. Alternatively, the thermal breakdown of detrital smectite that originated as weathered (oxidized) material would lead to reducing conditions and the precipitation of darkly luminescent calcite. In either case, succeeding generations of more luminescent carbonate would indicate a return to less-reducing conditions.

The final event documented in the Hoh rock assemblage is the precipitation of laumontite as discrete veins both along and cutting across foliation surfaces. Most laumontite veins were emplaced after the main phase of deformation in both the wall rocks and the fault zones, with the precipitation of laumontite largely controlled by the thrust-fault mélange and related structures. The Hoh rocks also have a progression of carbonate → carbonate+laumontite → laumontite veins, with equilibrium carbonate+laumontite occurring in numerous samples. In all cases, the laumontite and carbonate crystals contain no evidence of grain dissolution, and laumontite crystals can be found in predominantly carbonate veins (surrounded by carbonate) and vice versa. This coexistence of laumontite and carbonate indicates a high calcium activity and/or a low P_{CO_2} (Thompson, 1971). The progression of carbonate- to laumontite-dominated precipitation could be due to an increase in the calcium activity in the fluid phase, a decrease in the X_{CO_2}, or a change in the P-T conditions of the sample (Thompson, 1971). Decompression during late-stage uplift may have assisted in laumontite precipitation.

We observed no evidence for multiple precipitation events in the hanging-wall samples. Veins are also less common in these sections. The contrast between structural domains could be due to variations in sediment type, pore fluid, tectonic history, or may reflect a sampling bias, although fluid events were specifically targeted in all sections. Given the gross similarities in sediment type (clastic marine) and age, we suggest that the difference in recorded fluid activity may be due to structural setting. Upon thrust loading, the footwall would experience a dramatic increase in pressure, which could lead to fluid overpressuring, decreasing effective stress, and fracturing. Fracturing would provide a conduit for fluids to travel between the footwall and the fault zone. In contrast, the hanging wall would not experience thrust loading and overpressuring, and would not experience the fracturing necessary for significant fluid flow and vein precipitation.

Paragenetic Sequence and Deformational Events

The crosscutting relations between deformational features and fluid precipitates make it possible to relate the vein evolution to the

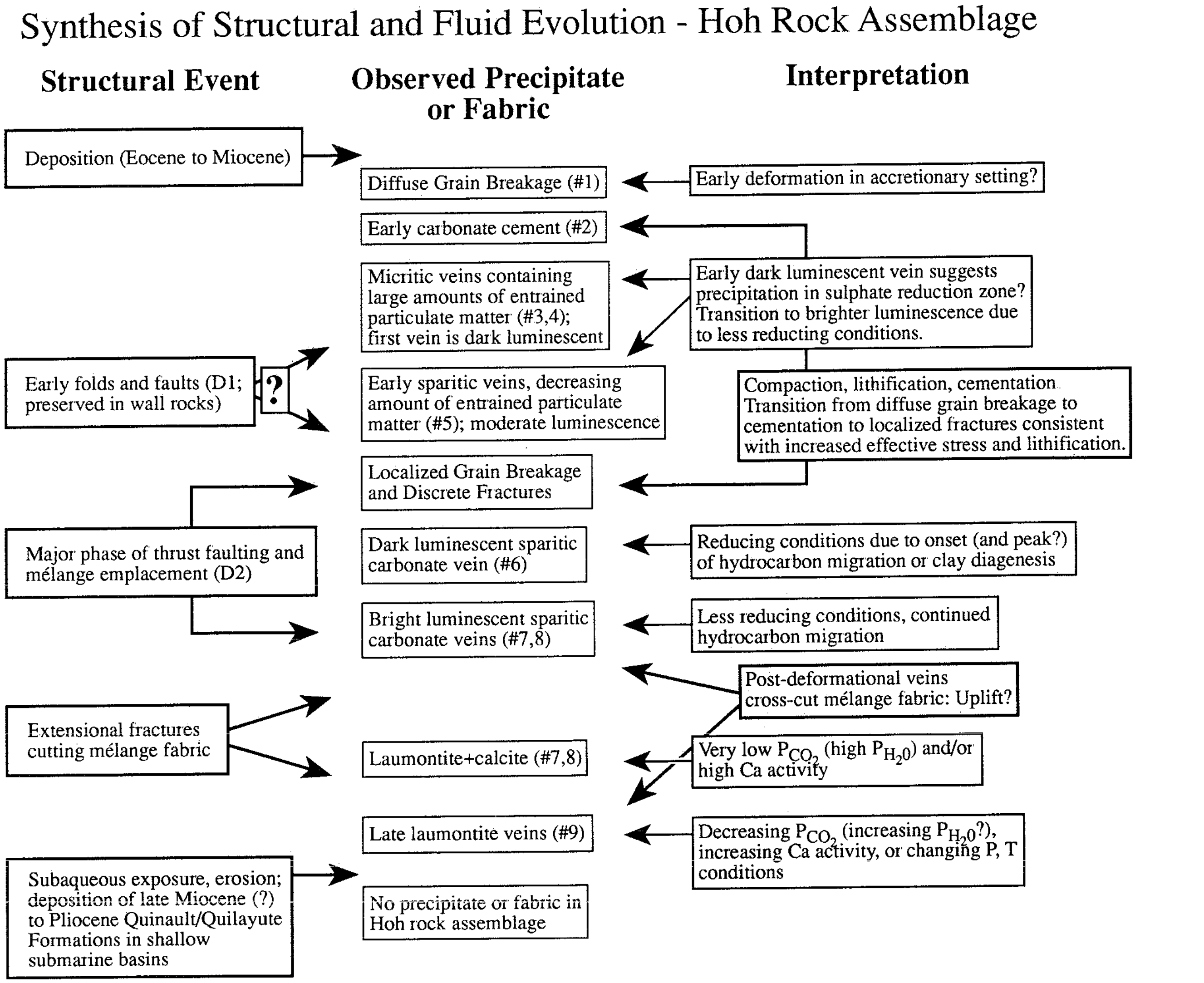

Figure 18. Combined structural history and paragenetic sequence for the Hoh rock assemblage, based upon crosscutting relationships between cements, veins, and deformational features.

tectonic history (Fig. 18). A large number of the samples display evidence of an early phase of distributed grain breakage. Optical and cathodoluminescence petrography indicate puzzle-piece fragments of identical luminescence commonly separated by matrix carbonate cement as well as undeformed mica grains isolated in the carbonate cement. These observations indicate that the distributed grain breakage occurred prior to the first phase of cementation. This matrix cementation is followed by a phase of localized cataclastic grain breakage.

The transition from distributed grain breakage (independent particulate flow) to localized cataclastic shear zones ("web structure" of Cowan, 1982; Byrne, 1984) requires an increase in the effective stress and/or an increase in density or degree of lithification (Fig. 18; Atkinson and Bramsby, 1978; Witschard and Dolan, 1990; Brown and Orange, in press). Whereas dewatering sediments will experience an increase in density, the presence of carbonate cement in the Hoh rocks indicates that increased lithification (cementation, consolidation) was also an important part of this transition. If cementation occurred during burial, then effective stress may also have played a role.

Not all cataclastic shear zones, however, are observed in samples that have carbonate cement. Severely deformed and cataclastically sheared graywacke sandstone has been noted in samples that lack evidence of carbonate cement. These samples may undergo the transition from distributed to localized grain breakage due to the increase in effective stress during burial and deformation, increase in density with dewatering, or to the increase in lithification due to reduced grain size, compaction, or cementation by a noncarbonate phase. On the basis of petrographic observations, this matrix material could be composed of clay particles rather than carbonate cement. In these samples, it is more difficult to place the deformation within the regional paragenetic sequence because of the lack of crosscutting relationships with visible fluid precipitates. These samples do indicate, however, that the cataclastic shear occurred during matrix mélange formation.

Cataclastic shear zones have been documented over a wide range of the paragenetic sequence, from prior to the earliest micritic veins (example: Hoh Head fault zone; Fig. 14) to after the last phase of lau-

Autochthonous Grey's Harbor, Chehalis Basins		Allochthonous Western Olympic Accretionary Complex
Galloway (1974) Depth or Temperature of Event		This Study
	Distributed Grain Breakage	Widespread Distributed Grain Breakage
z > 0 m	Calcite Pore Filling Cement	Calcite Cement: Pore Filling ± Alteration
z = 300 - 1500 m T = 10 - 60°C	Authigenic Clay Rims	Authigenic Clay Rims??
z = 1500 - 3500 m T = 45 - 90°C	Late Alteration Calcite	Calcite Veins
		Calcite ± Laumontite
z = 900 - 4600 m T = 45 - 70°C	Laumontite or Chlorite	Laumontite

Figure 19. Comparison of the paragenetic sequence documented in this study with the basinal studies of Galloway (1974). The late carbonate in the basinal samples precipitated over a wide range of the paragenetic sequence, whereas the relationship of clay diagenesis to the paragenesis of the Hoh rocks is poorly defined. Galloway determined the depths at which authigenic phases first appeared and the temperature gradients in these basins; the depths and inferred temperatures are shown here to provide a comparative framework for the Hoh rocks.

montite deposition (example: Teawhit footwall; Fig. 16). These two end members, however, are anomalous. The vast majority of cataclastic shear zones, specifically those related to matrix mélange deformation, formed after the bright, micritic veins (no. 5) and before the latest carbonate (nos. 7 and 8) and laumontite (no. 9) veins (see Summary; Fig. 17). These last carbonate and laumontite veins are also found undeformed along matrix foliation surfaces. This indicates that fluids utilized the fracture permeability as a fluid pathway, and that these veins precipitated after the main phase of matrix deformation.

Our observations of paragenetic events in samples from diverse structural levels and stratigraphic ages indicates that the sequential deposition of precipitates is regionally consistent, and that similar processes were active throughout the Hoh rock assemblage.

Paragenetic Sequence: Comparison with Nearby Basins

Galloway (1974) presented a study of the diagenetic evolution of graywacke sandstone within arc-related basins, including the Grays Harbor and Chehalis Basins of west-central Washington. The age of deposition in these basins overlaps that of the Hoh rocks (Eocene to Pliocene); the basinal sediments are similar to the Hoh rocks, except the latter contain more fine-grained material. These basins may be autochthonous analogs to the Hoh rocks.

All of the basins studied by Galloway (1974) contained a similar paragenetic sequence, which is compared to the Hoh rocks in Figure 19. "Mechanical crushing and compaction" occurred immediately after burial, followed by an early phase of calcite pore-filling cement. Subsequent diagenesis consisted of grain alteration and the coating of grains by authigenic clay, commonly chlorite and montmorillonite. The final stage of diagenesis consisted of a second period of cementation characterized by authigenic zeolite, typically laumontite, and/or phyllosilicate, either chlorite or montmorillonite. The relations between depth, heat flow, and diagenetic transitions led Galloway (1974) to postulate a temperature control for this paragenetic sequence. The depths and temperatures for the first appearance of authigenic phases documented by Galloway provide a framework for the thermal history of the Hoh rocks (Fig. 19).

The Hoh rocks contain a paragenetic sequence that is consistent with Galloway's work, yet Galloway presented data from cement only, whereas this study presents a sequence that includes cement and vein events. The Hoh rocks have an early phase of widespread distributed grain breakage and carbonate cementation similar to the basinal samples. In the Hoh rocks, the early cement is both an alteration product and a pore-filling cement. Graywacke sandstone in the Hoh also contains clay rinds on grains, and chloritic replacement of grains and matrix. The timing of these authigenic cements with respect to the overall paragenetic sequence is difficult to isolate and requires that grains with attached cements be present as inclusions within vein phases. In one of the few such relationships observed, dark sparitic carbonate veins within the Hoh Head fault zone contain grains that have a thin alteration rind. This rind appears to be clay (R. Garrison, 1991, personal commun.) and indicates that some alteration diagenesis occurred before mélange formation and syn-deformational vein emplacement. In general, however, the relations between clay diagenesis and the Hoh paragenetic sequence are poorly understood.

The late-stage laumontite veins in the Hoh rock samples correspond well with Galloway's paragenesis. Galloway, however, stated that this diagenetic phase is characterized by both laumontite and phyllosilicates, whereas the Hoh rocks contain only laumontite. Based upon field and well control, Galloway suggested that temperatures of at least 70–100 °C are required for laumontite precipitation (see also Juan, 1972; Murata and Whiteley, 1973), although more recent work by McCulloh and others (1978, 1981) indicates that laumontite may crystallize under strict T and P_{fluid} conditions at <32 and >200 °C. The coexistence of laumontite and calcite, however, implies enormous amounts of water (necessary to create an X_{CO_2} <

~0.01; Thompson, 1971), and temperatures less than ~275 °C.

CONCLUSIONS

The Hoh rock assemblage of the western Olympic Peninsula, Washington, contains sedimentary rocks of Eocene to Miocene age that were accreted to the continental margin, deformed, uplifted, and exposed by Pliocene time. This punctuated history of accretionary deformation contains no significant structural or thermal overprints, which allows for the in-depth examination of the tectonic and fluid evolution. The present exposure of the Hoh assemblage between La Push and the Hoh River includes thick (200–1,000 m) mélange fault zones and adjacent wall rocks. Wall rocks are folded and faulted, and many of the folds are oblique to, and are truncated by, the thrust faults, indicating that faulting postdated folding. The northwest-striking mélange zones are cut by a series of high-angle, northeast-striking faults that divide the field area into three distinct structural blocks. In each section, the matrix mélange fabric is intensely developed and closely spaced, dipping moderately to steeply to the northeast. Kinematic indicators indicate thrusting to the west-southwest.

The Hoh rock assemblage presents abundant evidence of fluid activity throughout its history. Petroliferous sandstone and matrix are associated with the mélange fault zones, and veins are a common feature in the mélange. Veins are more common in footwall samples, suggesting that tectonic loading led to fluid overpressures and the development of fractures in this section. The higher density and increased width of veins proximal to the fault zones may have been caused by increased strain adjacent to the fault zones (leading to increased fracturing) or by a higher fluid flux adjacent to the fault zones. The lower density of veins and the lack of multiple precipitation events in the hanging wall may be due to a lack of overpressuring in this section. Alternatively, the out-of-sequence thrusting represented by the mélange fault zones may have emplaced hanging-wall units that experienced a fluid evolution unrelated to the fault zones and footwall.

Paragenetic sequences assembled for samples from all structural levels in each of the three sections indicate a consistent progression of cements and veins over a strike distance of ~30 km. Early distributed grain breakage was followed by a period of carbonate cementation. Later deformation was accommodated by localized cataclastic shear and the development of web structure. A series of six carbonate veins postdate cementation, and the timing of the regional deformation may be accurately placed within this vein evolution.

The progression of carbonate precipitates within the Hoh rocks is from micritic to sparitic, as well as from early, dirty veins (abundant entrained particulate matter) to later, clear veins. The change in crystal size may be related to the decreasing salinity of fluids or the decreasing number of nucleation sites, whereas the change in crystal clarity may be due to the increasing cementation of the host sediment. The cathodoluminescence of carbonate also varies throughout the paragenetic sequence. The early cement is bright, and is crosscut by a dark micritic vein. This latter vein is interpreted to have precipitated in the presence of reducing fluids within the sulfate reduction zone, where excess Fe^{+2} may suppress the carbonate luminescence. The remaining six vein generations have an increasing luminescence, with the exception of a dark, sparitic vein midway through the vein history. This vein phase, common in all samples, may indicate that precipitation occurred under more reducing conditions due either to the onset of hydrocarbon migration or the breakdown of detrital smectite.

The main phase of thrusting in the mélange occurred after the precipitation of the micritic carbonate veins and before the precipitation of the bright, sparitic carbonate veins and laumontite. The later stages of veining included laumontite in equilibrium with calcite, whereas the last fluid precipitated a pure laumontite vein. The progression of precipitation events in the Hoh rocks is similar to that observed in autochthonous age-equivalent basins from western Washington, suggesting that the paragenetic sequence in the Hoh rock assemblage is neither a function of exotic fluids nor its accretionary setting.

ACKNOWLEDGMENTS

The authors wish to thank Parke Snavely, Jr. (U.S. Geological Survey) for whetting our appetite for Olympic geology and for initial support of this project. In addition, we owe a debt of gratitude to the Quinault and Quillayute Indian Nations for hospitality and for access to tribal lands. We would also like to thank the Olympic National Park for access and sampling permission. We thank Tim Walsh, Washington Department of Natural Resources, for XRD identification of laumontite. An earlier version of this manuscript benefitted from the comments of Bob Anderson and Eli Silver. Tim Byrne and Michael Underwood provided thorough reviews of the manuscript. This research was supported by National Science Foundation Grants EAR 88-10789 and EAR 90-05376 and a gift from the Weyerhaeuser Corporation. Acknowledgment is also made to the Donors of the Petroleum Research Fund, administered by the American Chemical Society, for support of this research (ACS PRF 23472-AC2).

APPENDIX. CORRESPONDENCE BETWEEN SAMPLE NUMBERS CITED AND ORANGE (1991)

This text	Orange (1991)
DO1	D88-3k-2
DO2	D88-4L-1a
DO3	D88-8h-2
DO4	D88-9i-1
DO5	D88-12g
DO6	D88-12g-3
DO7	D88-12g-4
DO8	D88-12h
DO9	D90-4e
DO10	D88-13a-2
DO11	D88-13a-3
DO12	D88-12m-3
DO13	D90-3d
DO14	D90-3e
DO15	D88-3d
DO16	D90-2e

REFERENCES CITED

Arnold, R., 1906, Geological reconnaissance of the coast of the Olympic Peninsula, Washington: Geological Society of America Bulletin, v. 17, p. 451–468.

Atkinson, J. H., and Bramsby, P. L., 1978, The mechanics of soils—An introduction to critical state soil mechanics: Maidenhead, England, McGraw-Hill, 375 p.

Barker, C. E., and Dalziel, M. C., 1991, Using cathodoluminescence to map regionally zoned carbonate cements occurring in diagenetic aureoles above oil reservoirs, Velma Oil Field, Oklahoma [abs.]: American Association of Petroleum Geologists Bulletin, v. 75, p. 538.

Bebout, G. E., 1991, Field-based evidence for devolatilization in subduction zones: Implications for arc magmatism: Science, v. 251, p. 413–416.

Bebout, G. E., and Barton, M. D., 1989, Fluid flow and metasomatism in a subduction zone hydrothermal system: Catalina schist terrane, California: Geology, v. 17, p. 976–980.

Blackwell, D. D., Bowen, R. G., Hull, D. A., Riccio, J., and Steele, J. L., 1982, Heat flow, arc volcanism, and subduction in northern Oregon: Journal of Geophysical Research, v. 87, p. 8735–8754.

Bray, C. J., and Karig, D. E., 1985, Porosity of sediments in accretionary prisms and some implications for dewatering processes: Journal of Geophysical Research, v. 90, p. 768–778.

Brown, K. M., and Orange, D. L., in press, Structural aspects of diapiric mélange emplacement: The Duck Creek diapir: Journal of Structural Geology, v. 15.

Byrne, T., 1984, Early deformation in mélange terranes of the Ghost Rocks Formation, Kodiak Islands, Alaska, *in* Raymond, L. A., ed., Mélanges: Their nature, origin, and significance: Geological Society of America Special Paper 198, p. 21–52.

Cowan, D. S., 1982, Origin of "vein structure" in slope sediments on the inner slope of the Middle America Trench off Guatemala, *in* Auboin, J., von Huene, R., and others, Initial reports of the Deep Sea Drilling Project, Volume 67: Washington, D.C., U.S. Government Printing Office, p. 645–650.

Cowan, D. S., and Potter, C. J., 1986, Centennial continent/ocean transect #9: Juan de Fuca spreading ridge to Montana thrust belt: Boulder, Colorado, Geological Society of America.

Davis, E. E., Hyndman, R. D., and Villinger, H., 1990, Rates of fluid expulsion across the northern Cascadia accretionary prism: Constraints from new heat flow and multichannel seismic reflection data: Journal of Geophysical Research, v. 95, p. 8869–8890.

DeMets, C., Gordon, R. G., Argus, D. F., and Stein, S., 1990, Current plate motions: International Geophysical Journal, v. 101, p. 425–478.

Engebretson, D. C., Cox, A., and Gordon, R. G., 1985, Relative motions between oceanic and continental plates in the Pacific basin: Geological Society of America Special Paper 206, 59 p.

Fisher, A. T., and Hounslow, M. W., 1990, Transient fluid flow through the toe of the Barbados accretionary complex: Con-

straints from Ocean Drilling Program Leg 110 heat flow studies and simple models: Journal of Geophysical Research, v. 95, p. 8845–8858.
Fisher, D., and Byrne, T., 1990, The character and distribution of mineralized fractures in the Kodiak Formation, Alaska: Implications for fluid flow in an underthrust sequence: Journal of Geophysical Research, v. 95, p. 9069–9080.
Folk, R. L., 1974, The natural history of crystalline calcium carbonate: Effect of magnesium content and salinity: Journal of Sedimentary Petrology, v. 44, p. 40–53.
Folk, R. L., and Land, L. S., 1975, Mg/Ca ratio and salinity: Two controls on crystallization of dolomite: American Association of Petroleum Geologists Bulletin, v. 59, p. 60–68.
Galloway, W. E., 1974, Deposition and diagenetic alteration of sandstone in northeast Pacific arc-related basins: Implications for graywacke genesis: Geological Society of America Bulletin, v. 85, p. 379–390.
Geddes, D., Orange, D. L., and Moore, J. C., 1990, Carbonate cement in sandstone as an indicator of accretionary complex hydrogeology: EOS (American Geophysical Union Transactions), v. 71, p. 1575.
Hansen, E. C., 1971, Strain facies: New York, Springer-Verlag, 207 p.
Juan, V. C., 1972, Epigenetic diagenesis and low grade metamorphism: Geological Society of China Proceedings, no. 15, p. 7–16.
Kastner, M., Elderfield, H., and Martin, J. B., 1991, Fluids in convergent margins: What do we know about their composition, origin, role in diagenesis and importance for oceanic chemical fluxes?: Royal Society of London Philosophical Transactions, ser. A, v. 335, p. 275–288.
Kingery, W. D., 1967, Introduction to Ceramics: New York, John Wiley and Sons, 781 p.
Koch, A. J., 1968, Petrology of the "Hoh Formation" of Tertiary age in the vicinity of the Raft River, western Washington [M.S. thesis]: Seattle, Washington, University of Washington, 41 p.
Kulm, L. D., von Huene, R., and others, 1973, Initial reports of the Deep Sea Drilling Project, Volume 18: Washington, D.C., U.S. Government Printing Office, 1,077 p.
Kulm, L. D., Peterson, C. P., Connard, G. G., Johnson, S. Y., Niem, W. A., McClain, K. J., Loubere, P. W., Lewis, B.T.R., Couch, R. W., Niem, A. R., Scheidegger, K. F., Crosson, R. S., and Stewart, R. J., 1984, Western North American continental margin and adjacent floor off Oregon and Washington: Woods Hole, Massachusetts, Atlas 1 Ocean Margin Drilling Program, Regional Atlas Series, Marine Sciences International, 32 sheets.
Kvenvolden, K. A., Rapp, J. B., Hostettler, F. D., and Snavely, P. D., Jr., 1989, Preliminary evaluation of the petroleum potential of the Tertiary accretionary terrane, west side of the Olympic Peninsula, Washington: Part 2—Comparison of molecular markers in oil and rock extracts: U.S. Geological Survey Bulletin 1892, p. 19–36.
Le Pichon, X., Iiyama, T., Boulegue, J., Charvet, J., Faure, M., Kano, K., Lallemant, S., Okada, H., Rangin, C., Taira, A., Urabe, T., and Uyeda, S., 1987, Nankai Trough and Zenisu Ridge: A deep submersible survey: Earth and Planetary Science Letters, v. 83, p. 285–299.
Lupton, C. T., 1914, Oil and gas in the western part of the Olympic Peninsula, Washington: U.S. Geological Survey Bulletin 581-B, p. 23–81.
Machel, H.-G., 1985, Cathodoluminescence in calcite and dolomite and its chemical interpretation: Geoscience Canada, v. 12, p. 139–147.
McCulloh, T. H., Cashman, S. M., and Stewart, R. J., 1978, Diagenetic baselines for interpretive reconstructions of maximum burial depths and paleotemperatures in clastic sedimentary rocks, *in* Oltz, D. F., ed., Low temperature metamorphism of kerogen and clay minerals: Society of Economic Paleontologists and Mineralogists, Pacific Section, Symposium in Geochemistry, p. 18–46.
McCulloh, T. H., Frizzell, V. A., Jr., Stewart, R. J., and Barnes, I., 1981, Precipitation of laumontite with quartz, thenardite, and gypsum at Sespe Hot Springs, western Transverse Ranges, California: Clays and Clay Minerals, v. 29, p. 353–364.
Meyers, W. J., 1974, Carbonate cement stratigraphy of the Lake Valley Formation (Mississippian), Sacramento Mountains, New Mexico: Journal of Sedimentary Geology, v. 44, p. 837–861.
Meyers, W. J., 1978, Carbonate cements: Their regional distribution and interpretation in Mississippian limestones of southwestern New Mexico: Sedimentology, v. 25, p. 371–400.
Moore, G., Shipley, T. H., Stoffa, P. L., Karig, D. E., Taira, A., Kuramoto, S., Tokuyama, H., and Suyehiro, K., 1990, Structure of the Nankai trough accretionary zone from multichannel seismic reflection data: Journal of Geophysical Research, v. 95, p. 8753–8765.
Moore, J. C., 1989, Tectonics and hydrogeology of accretionary prisms: Role of the décollement zone: Journal of Structural Geology, v. 11, p. 95–106.
Moore, J. C., and Sample, J. C., 1986, Mechanisms of accretion at sediment-dominated subduction zones: Consequences for the stratigraphic record and accretionary prism hydrogeology: Geological Society of Italy Memoir, v. 31, p. 107–118.
Moore, J. C., and others, 1988, Tectonics and hydrogeology of the northern Barbados Ridge: Results from Ocean Drilling Program Leg 110: Geological Society of America Bulletin, v. 100, p. 1578–1593.
Moore, J. C., Orange, D., and Kulm, L. D., 1990, Interrelationship of fluid venting and structural evolution: ALVIN observations from the frontal accretionary prism: Oregon: Journal of Geophysical Research, v. 95, p. 8795–8808.
Moore, J. C., Brown, K. M., Horath, F., Cochrane, G., MacKay, M., and Moore, G., 1991, Plumbing accretionary prisms: Effects of permeability variations: Royal Society of London Philosophical Transactions, ser. A, v. 335, p. 275–288.
Murata, K. J., and Whiteley, K. R., 1973, Zeolites in the Miocene Briones Sandstone and related formations of the central Coast Ranges, California: U.S. Geological Survey Journal of Research, v. 1, p. 255–265.
Orange, D. L., 1990, Criteria helpful in recognizing shear zone and diapiric mélanges: Examples from the Hoh Accretionary Complex, Olympic Peninsula, Washington: Geological Society of America Bulletin, v. 102, p. 935–951.
Orange, D. L., Knittle, E., Farber, D., and Williams, Q., 1990, Spectroscopic studies of hydrocarbon fluid inclusions in calcite: Implications for fluid evolution of the Hoh accretionary complex, Olympic Peninsula, Washington: PACROFI III: Third Biennial Pan-American Conference on Research on Fluid Inclusions, May 20–22, 1990, Toronto, Ontario, Canada, p. 67.
Palmer, R. H., 1927, The Hoh Formation of Washington: Journal of Geology, v. 35, p. 276–278.
Rau, W. W., 1970, Foraminifera, stratigraphy, and paleoecology of the Quinault Formation, Point Grenville–Raft River coastal area, Washington: Washington Department of Natural Resources Bulletin no. 62, 41 p.
Rau, W. W., 1973, Geology of the Washington Coast between Point Grenville and the Hoh River: Washington Department of Natural Resources, Geology and Earth Resources Division, Bulletin no. 66, 58 p.
Rau, W. W., 1975, Geologic map of the Destruction Island and Taholah quadrangles, Washington: Olympia, Washington, Washington Department of Natural Resources, scale 1:62,500.
Rau, W. W., 1979, Geologic map in the vicinity of the Lower Bogachiel and Hoh Rivers, and the Washington Coast: Washington Department of Natural Resources, Division of Geology and Earth Resources, Geologic Map GM-24.
Rau, W. W., 1980, Washington coastal geology between the Hoh and Quillayute Rivers: Washington Department of Natural Resources Bulletin No. 72, 57 p.
Rau, W. W., and McFarland, C. R., 1982, Coastal wells of Washington: Washington Division of Geology and Earth Resources Report of Investigations 26, 4 sheets.
Reagan, A. B., 1909, Some notes on the Olympic Peninsula, Washington: Kansas Academy of Sciences Transactions, v. 22, p. 131–238.
Riddihough, R. P., 1977, A model for recent plate interactions off Canada's west coast: Canadian Journal of Earth Sciences, v. 14, p. 384–396.
Seely, D. R., 1977, The significance of landward vergence and oblique structural trends on trench inner slopes, *in* Talwani, M., and Pitmann, S. C., eds., Island arcs, deep sea trenches, and back-arc basins: American Geophysical Union, Maurice Ewing Series 1, p. 187–198.
Silver, E. A., 1972, Pleistocene tectonic accretion of the continental slope off Washington: Marine Geology, v. 13, p. 239–249.
Snavely, P. D., Jr., 1987, Tertiary geologic framework, neotectonics, and petroleum potential of the Oregon-Washington continental margin, *in* Scholl, D. W., Grantz, A., and Vedder, J. G., eds., Geology and resource potential of the continental margin of western North America and adjacent ocean basins—Beaufort Sea to Baja California: Houston, Texas, Circum-Pacific Council for Energy and Mineral Resources, Earth Science Series, v. 6, p. 305–335.
Snavely, P. D., Jr., and Kvenvolden, K. A., 1989, Preliminary evaluation of the petroleum potential of the Tertiary accretionary terrane, west side of the Olympic Peninsula, Washington: Part 1—Geology and hydrocarbon potential: U.S. Geological Survey Bulletin 1892, p. 1–18.
Snavely, P. D., Jr., and Wagner, H. C., 1982, Geologic cross section across the continental margin of southwestern Washington: U.S. Geological Survey Open-File Report 82-459, 10 p.
Speed, R., 1990, Volume loss and defluidization history of Barbados: Journal of Geophysical Research, v. 95, p. 8983–8996.
Stewart, R. L., 1970, Geologic map of the Hoh River–Queets River area, Olympic Peninsula, Washington [M.S. thesis]: Seattle, Washington, University of Washington, 74 p.
Stewart, R. J., 1974, Zeolite metamorphism of sandstone in the western Olympic Peninsula, Washington: Geological Society of America Bulletin, v. 85, p. 1139–1142.
Tabor, R. W., and Cady, W. M., 1978a, The structure of the Olympic Mountains, Washington—Analysis of a subduction zone: U.S. Geological Survey Professional Paper 1033, 38 p.
Tabor, R. W., and Cady, W. M., 1978b, Geologic map of the Olympic peninsula, Washington: U.S. Geological Survey Miscellaneous Investigations Series, Map I-994, 2 sheets, scale 1:125,000.
Thompson, A. B., 1971, P CO2 in low-grade metamorphism: Zeolite, carbonate, clay mineral, prehnite relations in the system CaO-Al203-SiO2-CO2-H2O: Contributions to Mineralogy and Petrology, v. 33, p. 145–161.
Torrini, R., Jr., Speed, R. C., and Matoili, G. S., 1985, Tectonic relationships between forearc basin strata and the accretionary complex at Bath, Barbados: Geological Society of America Bulletin, v. 96, p. 861–874.
Tucker, M. E., 1981, Sedimentary petrology: An introduction: New York, Halsted Press, John Wiley and Sons, 252 p.
Underwood, M. B., Shelton, K. L., Laughland, M. M., Clendenen, W., and Heizler, M., 1989, Thermal maturity and fluid-rock interactions, Franciscan accretionary complex, Big Sur, California: Geological Society of America Abstracts with Programs, v. 21, p. A338.
Underwood, M. B., Laughland, M. M., Byrne, T., Hibbard, J., and DiTullio, L., 1992, Thermal evolution of the Tertiary Shimanto Belt, Muroto Peninsula, Shikoku, Japan: The Island Arc, v. 1, p. 116–132.
Vrolijk, P., Myers, G., and Moore, J. C., 1987, Warm fluid migration along tectonic mélanges in the Kodiak accretionary complex, Alaska: Journal of Geophysical Research, v. 93, p. 10313–10324.
Vrolijk, P., Fisher, A., and Gieskes, J., 1992, Geochemical and geothermal evidence for fluid migration in the Barbados accretionary prism (ODP Leg 110): Geophysical Research Letters, v. 18, p. 947–950.
Wagner, H. C., Batatian, L. D., Lambert, T. M., and Tomson, J. H., 1986, Preliminary geologic framework studies showing bathymetry, locations of geophysical tracklines and exploratory wells, sea floor geology and deeper geologic structures, magnetic contours, and inferred thickness of Tertiary rocks on the continental slope off southwestern Washington between latitudes 46N and 48.5N and from the Washington coast to 125.33W: Washington Department of Natural Resources, Division of Geology and Earth Resources, Open-File Report 86-1.
Weaver, C. E., 1937, Tertiary stratigraphy of western Washington and north-western Oregon: University of Washington Publications in Geology, v. 4, 266 p.
Westbrook, G. K., and Smith, M. J., 1983, Long décollements and mud volcanoes: Evidence from the Barbados Ridge Complex for the role of high pore-fluid pressure in the development of an accretionary complex: Geology, v. 11, p. 279–283.
Witschard, M., and Dolan, J. F., 1990, Contrasting structural styles in siliciclastic and carbonate rocks of an offscraped sequence: The Peralta accretionary prism, Hispaniola: Geological Society of America Bulletin, v. 102, p. 792–806.

Manuscript Received by the Society August 16, 1991
Revised Manuscript Received February 2, 1993
Manuscript Accepted February 9, 1993

Printed in U.S.A.